



## OPEN ACCESS

## EDITED BY

Ghazala Muteeb,  
King Faisal University, Saudi Arabia

## REVIEWED BY

Ajay Singh Tanwar,  
ST Jude Children's Research Hospital,  
United States  
Sharanabasava V. Ganachari,  
KLE Technological University, India

## \*CORRESPONDENCE

Regina Sharmila Dass,  
✉ reginadass@gmail.com

RECEIVED 11 April 2023

ACCEPTED 25 July 2023

PUBLISHED 10 August 2023

## CITATION

Kanak KR, Dass RS and Pan A (2023), Anti-quorum sensing potential of selenium nanoparticles against LasI/R, RhII/R, and PQS/MvfR in *Pseudomonas aeruginosa*: a molecular docking approach. *Front. Mol. Biosci.* 10:1203672. doi: 10.3389/fmolb.2023.1203672

## COPYRIGHT

© 2023 Kanak, Dass and Pan. This is an open-access article distributed under the terms of the [Creative Commons Attribution License \(CC BY\)](https://creativecommons.org/licenses/by/4.0/). The use, distribution or reproduction in other forums is permitted, provided the original author(s) and the copyright owner(s) are credited and that the original publication in this journal is cited, in accordance with accepted academic practice. No use, distribution or reproduction is permitted which does not comply with these terms.

# Anti-quorum sensing potential of selenium nanoparticles against LasI/R, RhII/R, and PQS/MvfR in *Pseudomonas aeruginosa*: a molecular docking approach

Kanak Raj Kanak<sup>1</sup>, Regina Sharmila Dass<sup>1\*</sup> and Archana Pan<sup>2</sup>

<sup>1</sup>Fungal Genetics and Mycotoxicology Laboratory, Department of Microbiology, School of Life Sciences, Pondicherry University (A Central University), Pondicherry, India, <sup>2</sup>Department of Bioinformatics, School of Life Sciences, Pondicherry University (A Central University), Pondicherry, India

*Pseudomonas aeruginosa* is an infectious pathogen which has the ability to cause primary and secondary contagions in the blood, lungs, and other body parts of immunosuppressed individuals, as well as community-acquired diseases, such as folliculitis, osteomyelitis, pneumonia, and others. This opportunistic bacterium displays drug resistance and regulates its pathogenicity via the quorum sensing (QS) mechanism, which includes the LasI/R, RhII/R, and PQS/MvfR systems. Targeting the QS systems might be an excellent way to treat *P. aeruginosa* infections. Although a wide array of antibiotics, namely, newer penicillins, cephalosporins, and combination drugs are being used, the use of selenium nanoparticles (SeNPs) to cure *P. aeruginosa* infections is extremely rare as their mechanistic interactions are weakly understood, which results in carrying out this study. The present study demonstrates a computational approach of binding the interaction pattern between SeNPs and the QS signaling proteins in *P. aeruginosa*, utilizing multiple bioinformatics approaches. The computational investigation revealed that SeNPs were acutely 'locked' into the active region of the relevant proteins by the abundant residues in their surroundings. The PatchDock-based molecular docking analysis evidently indicated the strong and significant interaction between SeNPs and the catalytic cleft of LasI synthase (Phe105-Se = 2.7 Å and Thr121-Se = 3.8 Å), RhII synthase (Leu102-Se = 3.7 Å and Val138-Se = 3.2 Å), transcriptional receptor protein LasR (Lys42-Se = 3.9 Å, Arg122-Se = 3.2 Å, and Glu124-Se = 3.9 Å), RhIR (Tyr43-Se = 2.9 Å, Tyr45-Se = 3.4 Å, and His61-Se = 3.5 Å), and MvfR (Leu208-Se = 3.2 Å and Arg209-Se = 4.0 Å). The production of acyl homoserine lactones (AHLs) was inhibited by the use of SeNPs, thereby preventing QS as well. Obstructing the binding affinity of transcriptional regulatory proteins may cause the suppression of LasR, RhIR, and MvfR systems to become inactive, thereby blocking the activation of QS-regulated virulence factors along with their associated gene expression. Our findings clearly showed that SeNPs have anti-QS properties against the established QS systems of *P. aeruginosa*, which strongly advocated that SeNPs might be a potent solution to tackle drug resistance and a viable alternative to conventional antibiotics along with being helpful in therapeutic development to cure *P. aeruginosa* infections.

## KEYWORDS

antimicrobial resistance, *in silico* drug design, molecular docking, microbial nanoparticle interaction, PatchDock, *Pseudomonas aeruginosa*, quorum sensing, selenium nanoparticles

## 1 Introduction

*Pseudomonas aeruginosa* is an example of an opportunity-driven infectious bacterium, which is Gram-negative in its natural state. This nosocomial bacterial infection is a prominent cause of a variety of illnesses. It spreads easily in healthcare settings. These germs are responsible for approximately 10% of nosocomial bacterial infections (Gellatly and Hancock, 2013). Immunocompromised patients are at a higher risk of contracting a nosocomial infection (Dye, 2014). *P. aeruginosa* targets individuals with burn wounds, chronic obstructive pulmonary disorder (COPD), cancer, cystic fibrosis, immunodeficiency, and severe infections requiring ventilation (such as COVID-19) and poses a particular challenge in intensive care units (ICUs) (Raman et al., 2018; Lansbury et al., 2020; Killough et al., 2022; Qin et al., 2022). *P. aeruginosa*, with its diverse set of virulence factors and innate adaptation to different conditions, is responsible for a slew of severe, possibly deadly acute and chronic infections, particularly in immunocompromised hosts, where fatality rates may exceed 40%. It is a lethal hazard to immunocompromised individuals. It is the most significant cause of bacteremia and sepsis in neutropenic cancer patients receiving chemotherapy and the predominant cause of hospital-acquired pneumonia and respiratory failure (Osmon et al., 2004; Matos et al., 2018; Killough et al., 2022; Wood et al., 2023). *P. aeruginosa* infections are also prevalent in surgical wounds, corneal, and diabetic ulcers. Additionally, there is a growing incidence of life-threatening *P. aeruginosa* infections in AIDS patients (Shepp et al., 1994; Wood et al., 2023).

*P. aeruginosa* adopts a biofilm mode of existence in which it evolves extreme persistency to both antibiotics and immune defense cascade, leading to multidrug resistance as a consequence of excessive selective pressure from uncontrolled consumption of conventional antibiotics (Su et al., 2010; Abinaya and Gayathri, 2019). *P. aeruginosa* is resistant to numerous antibiotics, such as aminoglycosides, quinolones, and lactams (Pang et al., 2019). In general, the strategies used by *P. aeruginosa* to resist antibiotics can be categorized as intrinsic, acquired, or adaptive resistance. Low outer membrane permeability, the expression of efflux pumps that eject antibiotics out of the cell, and the synthesis of antibiotic-inactivating enzymes comprise an intrinsic resistance approach of *P. aeruginosa*. *P. aeruginosa* can achieve acquired resistance through horizontal transmission of resistant genes or mutational alterations (Breidenstein et al., 2011). Adaptive resistance, on the other hand, is characterized by the growth of biofilms in the infected patients, which act as barriers limiting antibiotic penetration to the bacterial cells (Drenkard, 2003). This adaptive resistance enhances the survival of the bacterium against antibiotic assaults by transiently modifying gene and/or protein expression in response to environmental stimuli, and it can be reversed once the stimulus is removed (Sandoval-Motta and Aldana, 2016). Furthermore, within the biofilm, there is the development of multidrug-tolerant persister cells that can withstand antibiotic attacks, contributing to prolonged and persistent infections in affected

patients. Among the various mechanisms, the formation of biofilms and the generation of persister cells are the most extensively studied aspects of adaptive resistance in *P. aeruginosa*, leading to persistent infections and unfavorable prognoses in affected individuals (Taylor et al., 2014).

The general mechanisms of biofilm-mediated resistance protecting bacteria from antibiotic attack involve the prevention of antibiotic penetration, altered microenvironment inducing slow growth of biofilm cells, and expression of an adaptive stress response permitting survival under harsh conditions that stimulate and alter the chemical microenvironment within the biofilm, which induces slow growth of bacteria, resulting as the reduction of antibiotic uptake and formation of multidrug-tolerant persister cells (Stewart, 2002; Balaban et al., 2013). Persister cells do not proliferate in the presence of antibiotics; however, they resume growth once the antibiotics are removed (Maisonneuve and Gerdes, 2014). Furthermore, environmental stimuli have an impact on the formation and proliferation of persister cells. Moreover, the quorum sensing (QS) signaling molecule acyl-homoserine lactone 3-OC12-HSL has been reported to greatly increase the number of persister cells in *P. aeruginosa* cultures (Moker et al., 2010; Mlynarcik and Kolar, 2017).

The pathogenic features of *P. aeruginosa* are modulated by a cell concentration-based process known as QS that utilizes QS molecules. The QS system is a bacterial intercellular signaling mechanism that is governed by the discharge of diffusible chemical compounds known as autoinducers (Reading and Sperandio, 2006; Banik et al., 2009) that are recognized by a receptor. These QS molecules regulate a number of detrimental behaviors in both the Gram-negative and positive bacteria, including an assembly of virulence factors and the biofilm generation (Davies, 2003). The bacterial regulatory system known as QS is involved in controlling an array of cellular cascading display, including the production of antibiotics, biofilm production, bioluminescence, competence, sporulation, and the secretion of virulence factors (Moghaddam et al., 2014). QS signaling is also employed by *P. aeruginosa* to control the expression level of genes and play an important role in its pathogenic activity (Smith and Iglewski, 2003).

Reportedly, *P. aeruginosa* possesses four interconnected QS signaling networks, namely, LasI/LasR, RhlI/RhlR, *Pseudomonas* quinolone signal (PQS)/MvfR, and IQS (integrated QS). Within these networks, LasI and RhlI synthase enzymes activate the Las and Rhl pathways, which are responsible for producing acyl homoserine lactone (AHL) signaling molecules, such as 3-oxododecanoyl-l-homoserine lactone (3-oxo-C12-HSL) and butyryl-l-homoserine lactone (C4-HSL), respectively (Lee and Zhang, 2015; Rampioni et al., 2016). These molecules, 3-oxo-C12-HSL and C4-HSL, bind and activate their respective transcription factors, LasR and RhlR, triggering biofilm formation and the expression of various virulence factors, such as elastase, proteases, pyocyanin, lectins, rhamnolipids, and toxins (Rutherford and Bassler, 2012). The initiation of the third QS system occurs by the transcriptional regulator MvfR (PqsR) by binding to 2-heptyl-3-hydroxy-4(1H)-quinolone, which is a PQS

signaling molecule (Déziel et al., 2005), to promote biofilm formation. The PQS-MvfR system controls the production of the *Pseudomonas* quinolone signal (PQS) through the regulation of the pqsABCDE operon by the transcriptional regulator MvfR, also known as PqsR. These PQS signaling molecules work in the absence or dysfunction of LasR and activate the virulence genes (Lee and Zhang, 2015). Lee and co-workers (2013) suggested a novel QS molecule, namely, 2-(2-hydroxyl-phenyl)-thiazole-4-carbaldehyde, which constituted a fourth QS system, i.e., IQS (Lee et al., 2013). However, since its discovery, there has been debate over IQS, and the specific role of the IQS molecule in the QS system requires further exploration (Lee and Zhang, 2015; Lin and Cheng, 2019). We are excluding IQS from the current analysis due to the lacuna of reliable data about the process of IQS creation and their significance in the QS system (Cornelis, 2020). As a result, only the inhibitory potential of selenium nanoparticles (SeNPs) against the Las, Rhl, and PQS QS systems was studied in the present investigation and analysis.

*P. aeruginosa* manages their contained virulence by generating, perceiving, and reacting to autoinducers, which are extracellular signaling molecules that attach to a receptor (Rutherford and Bassler, 2012; Longo et al., 2013). Investigations concerning *P. aeruginosa*-based QS signaling molecules indicate that these autoinducers (AHLs) influence the synthesis of virulence factors and their relative consequences (Pearson et al., 1997; Van Delden and Iglewski, 1998; Pesci et al., 1999). When homo serine lactones and PQS autoinducers are present at optimal concentrations, they bind to specific receptor proteins, namely, LasR, RhlR, and MvfR, and stimulate the transcription of numerous genes responsible for producing various virulence factors, such as elastases, pyocyanin, rhamnolipids, and siderophores (Passador et al., 1993; Strateva and Mitov, 2011; Moradali et al., 2017). In *P. aeruginosa*, these QS signaling molecules are liable for infection; thus, proteins implicated in QS signaling could be serving as potential targets to develop antimicrobial agents. Although antibiotics are available to treat the illness, the combined effect of the QS complex causes infection; nevertheless, the antibiotic treatment is ineffectual since resistance develops in a short amount of time, making this bacterium a serious threat (Juan et al., 2010; Su et al., 2010; Ali et al., 2017; Abinaya and Gayathri, 2019). Reports suggested that a defect in QS systems renders *P. aeruginosa* less virulent and also results in the production of a flat biofilm that is susceptible to antibiotics (Jensen et al., 2007; Van Gennip et al., 2009). Therefore, disrupting these bacterial QS systems could be beneficial in the treatment of various diseases due to the fact that QS molecules are instrumental in controlling virulence (Alvarez et al., 2012). Thus, inhibiting quorum sensing is regarded as a promising strategy for combating *P. aeruginosa* infections (Hurley et al., 2012). This approach can effectively prevent biofilm formation, diminish bacterial virulence, and carry a low risk of provoking bacterial resistance (Reuter et al., 2016). Moreover, this strategy exhibits a narrow spectrum, making it unlikely to inadvertently inhibit beneficial bacteria (Pang et al., 2019). As a result, a cost-effective and alternative therapy to treat *P. aeruginosa* infection is required. Moreover, the development of new antibiotics is very limited and time consuming. Thus, the development of novel therapeutic

approaches to treat *P. aeruginosa* infections is highly desirable and has gained much attention in the past decade (Hurley et al., 2012; Chatterjee et al., 2016).

Nanoparticles could potentially interrupt QS molecules, allowing nanotechnology to provide a solution to this problem. Additionally, nanoparticles have the benefits of reducing toxicity, conquering resistance, and being more economical (Pal et al., 2007; Weir et al., 2008). Mühlhling and coworkers evidenced that native habitat bacteria have no resistance to nanoparticles (Mühlhling et al., 2009). As a result, several researchers have begun to use nanotechnology to generate advanced versions of antimicrobials, such as QS-targeted nano-inhibitors, in recent years. The approaches under this field could lead to benefits such as enhanced coating and dispersion of biofilms, increased solubility, ease of administration, and the maintenance of QS inhibitor activity (Nafee et al., 2014). In this regard, the production of bio-metallic nanoparticles is an emerging route as a potential, environmentally accessible, and nontoxic alternative to chemical or physical synthesis of nanoparticles. The antimicrobial activity of numerous nanoparticles has been reported in the past few years, including silver, gold, polymeric, and tin oxide nanoparticles, all of which have various modes of action (Samanta et al., 2017; Al-Shabib et al., 2018; Flockton et al., 2019). Only few scientific studies have demonstrated the inhibitory potential of SeNPs to QS-mediated virulence factors and that they have anti-biofilm function (Singh et al., 2017; Gómez-Gómez et al., 2019). Various accounts proclaiming NPs to be anti-QS agents exist, yet only a few studies have concentrated on the mechanistic approach and computational analysis of SeNPs to discover the possibility of them becoming anti-QS agents (Singh et al., 2017; Gómez-Gómez et al., 2019). Considering the significance of computational analysis and the scarcity of literature on the mechanics of SeNPs interacting with QS-controlled virulence genes, we set out to accomplish a few objectives: 1) computational investigation to check the potential of SeNPs as an anti-QS agent, 2) analysis of binding between SeNPs and QS-regulatory proteins, i.e., the LasI/RhlI-based AHL synthase, using the molecular docking approach, 3) to optimize the bonding between SeNPs and LasR/RhlR, a transcriptional regulatory protein in QS of *P. aeruginosa* using molecular docking, and 4) assessment of the residual-binding pattern between SeNPs and a PQS signaling receptor protein MvfR, using protein–ligand docking.

## 2 Materials and methods

### 2.1 Retrieval of the protein sequences and homology modeling

The crystallographic 3D structural design of the three key QS proteins LasI synthase, transcriptional activator protein LasR, and MvfR transcriptional protein with their respective PDB IDs 1RO5 (resolution = 2.3 Å), 2UV0 (chain E, resolution = 1.8 Å), and 4JVC (resolution = 2.5 Å) was retrieved from the Protein Data Bank (PDB; [www.rcsb.org](http://www.rcsb.org)). However, the PDB did not contain the 3D crystal structures of two other QS-related proteins, i.e., RhlI synthase and RhlR. Therefore, homology modeling was carried out in order to model the 3D structures of each of these proteins. The RhlI synthase and RhlR amino acid sequences were obtained from the National

Centre for Biotechnology Information (NCBI) (<http://www.ncbi.nlm.nih.gov/>) and stored as a FASTA file with the corresponding accession numbers P54291.2 and AAC44036.1, respectively, as the query sequence and employed for homology modeling. The tertiary structure of RhlI synthase and RhlR was predicted by homology modeling in the Robetta server (Raman et al., 2009; Song et al., 2013). Robetta (<http://robetta.bakerlab.org>) is a web-based platform that offers automated estimation of structure and analysis tools for inferring protein structural characteristics from genomic sequences. The service makes use of the first completely automated structure forecasting approach, which generates a model for a whole protein sequence irrespective of whether it overlaps or not its sequence homology with protein(s) whose structures are already known. Robetta creates structural models of proteins by parsing the protein sequence into potential domains. Robetta protein modeling utilizes both comparative modeling, which is employed when a suitable template match is found, and *de novo* modeling, which is used when a suitable template match is not available. In this study, PSI-BLAST was employed to perform amino acid sequence alignment, and the top 20 hits with the highest identity were chosen as templates for further investigation.

## 2.2 Structure model evaluation and validation

The selected homology model was evaluated for its compatibility with different structural variables using reliable and comparable assessment tools, such as WHAT IF, PROCHECK, ERRAT, and VERIFY-3D. These tools were employed to assess and verify different aspects of the structural quality of the model. The final structure of the modeled protein was analyzed by the WHAT IF server (Vriend, 1990) followed by the SAVES server (<http://nihserver.mbi.ucla.edu/SAVES/>). The stereochemical accuracy with the overall structural geometry of the modeled protein was evaluated and confirmed using PROCHECK, a program that evaluates the stereochemical quality of protein structures (Laskowski et al., 1993). A structure evaluation server, VERIFY-3D (Lüthy et al., 1992), was utilized to evaluate the compatibility of the structure of the model and its corresponding amino acid residues, which assigned a structural class to the model considering its location and surroundings. In addition, ERRAT graphs were generated to further evaluate the compatibility of the model. Ramachandran plot statistics were analyzed using the online server RAMPAGE to evaluate the stability of the model. Furthermore, Ramachandran plot analysis was implemented to evaluate the complete stereochemical content of the protein and the amino acid residues in the permitted and disallowed regions.

## 2.3 Molecular dynamics simulation of the modeled proteins

The best-scored modeled tertiary structure of the RhlI synthase and RhlR obtained from the Robetta server was chosen for further study. Molecular dynamics simulations were conducted to assess the stability of the modeled protein using GROMACS 2019 with the GROMOS 54a7 force field. The simulations were carried out for a

duration of 100 nanoseconds (ns) in a cubic box with a size of 1.0 nanometer (nm). The box was loaded with simple point charges, and four Na<sup>+</sup> ions were introduced to neutralize the system. For neutralization, the solvent molecule was replaced with Na<sup>+</sup> ions in the SPC/E water model. A periodic boundary condition was implemented in every possible direction. The predicted models underwent energy minimization with a maximum of 50,000 steps employing the conjugate gradient algorithm and steepest descent minimization. The minimization process terminated when the force was below 1000.0 kJ/mol/nm. Subsequently, each system was equilibrated for 1000 picoseconds (ps) under NVT and NPT ensemble with constant number of their respective particles, volume, temperature, and pressure employing a Berendsen thermostat. The partial mesh Ewald algorithm was used to estimate the electrostatic and van der Waals interactions, with the short-range neighbor list cut-off, short-range electrostatic cut-off, and short-range van der Waals cut-off all set to 1 nm. The particle mesh Ewald method was employed for ensemble generation with a cut-off of 10. To ensure a steady environment, temperature at 300 K and pressure coupling at 1 bar were employed, with coupling values set to 2 and 0.1 ps, respectively. The compressibility was set to 4.5 e<sup>-5</sup>/bar. The whole setup underwent equilibration for 500 and 100 ps using NVT and NPT ensembles, respectively. Last, the equilibrated system was simulated without constraints for 100 ns with a time step of 2 fs using the NPT ensemble to explore the structural dynamics of the modeled proteins. GROMACS utility packages, such as *g\_rms* and *g\_rmsf*, were used to compute root-mean-square deviation (RMSD) and root-mean-square fluctuation (RMSF) for the homology model trajectories at 100 ns. All graphs were created using the GRACE software (<http://plasma-gate.weizmann.ac.il/Grace/>). RMSD amid the main-chain atom of model proteins between pre-simulation and post-simulation was determined by superimposition using PyMol (version 4.6.0).

## 2.4 Preparation of the ligand molecule

### 2.4.1 Preparation of the 3D structure of SeNPs

The structure of the SeNPs was extracted using the PubChem database (<https://www.ncbi.nlm.nih.gov/pccompound>) in the *.sdf* data file format. Additionally, the conversion of 2D to 3D structures was carried out by using MarvinSketch (ver.15.11.30) and saved as a *.pdb* data file.

## 2.5 Molecular docking analysis

### 2.5.1 Prediction of the docking or active site of Las, Rhl, and PQS systems

The CASTp tool was employed to predict the binding sites of SeNPs for the generated LasI/R and RhlI/R models along with MvR protein. The *.pdb* files were uploaded into the tool, and subsequent processing of these files enabled the selection of active binding sites for SeNP ligands.

### 2.5.2 Molecular docking

Molecular docking was carried out using the rigid protein structures of the LasI synthase, LasR receptor, RhlI synthase, and

RhlR receptor. Specifically, the interaction between SeNPs and LasI (AHL synthase), as well as LasR/MvfR (transcriptional receptor proteins), was examined separately using the PatchDock online program. The interactions of SeNPs with the AHL synthase LasI, LasR receptor, and AHL assess long-range electrostatic interactions. The synthase RhlI and RhlR receptor, along with PQS receptor MvfR, were examined and explored with the assistance of the PatchDock tool (Schneidman-Duhovny et al., 2005). The protein files were modified by removing water molecules along with their native ligand. Ligand files were prepared according to the specifications of the tool, and default docking parameters were maintained. PatchDock, a geometry-based molecular docking algorithm, which has been critically assessed by the CAPRI initiative, was employed. PatchDock detects the most efficient protein–ligand interacting partner by assessing the conformational compatibility of flexible molecular interfaces. The RMSD clustering value for this parameter was kept at 4 Å as the default parameter recommended by the tool. In the post-docking process, the docking geometric score, desolvation energy, and ligand-interacting amino acids of the QS regulator proteins were evaluated using the output of the result provided from the PatchDock service. The scores of the docked files were then selected based on their ranking, and the figures were visualized using PyMol 3D visualization software (DeLano, 2002).

### 3 Results and discussion

SeNPs have low toxicity and great biocompatibility. As a result, they have attracted a great deal of interest with adoption in the biomedicine and food business organizations (Tran et al., 2015; Gunti et al., 2019). Selenium is an essential component in the production of selenoproteins, which include important antioxidants, such as deiodinase, glutathione peroxidase, and thioredoxin reductase (Rotruck et al., 1973). This is considered an essentially required trace element for the upkeep of human health, and the recommended amount of selenium in an adult's daily dietary supplement ranges from 40 to 400 µg (Arthur, 1991; Rayman, 2005). Consequentially, the use of SeNPs is extremely acceptable and recommended in pharmaceutical and food industries. Among its many beneficial properties, SeNPs are an important metalloids trace element that possesses notable antimicrobial, antioxidant, and anticarcinogenic potential. Furthermore, previous studies have shown that SeNPs synthesized through biological means exhibit anti-QS and antibiofilm properties against numerous pathogens (Singh et al., 2017). The research team also demonstrated the antibiofilm potential of selenium nanovectors and showed masked interest in the interaction of SeNPs with the LasR QS protein. However, there needs to be more *in silico* findings on the association of SeNPs with Las, Rhl, and PQS regulatory proteins associated with the *P. aeruginosa* QS system. Therefore, we adopted an *in silico* method to conduct exploratory research into the QS-modulatory mechanism of SeNPs. It is generally agreed upon that *P. aeruginosa* makes use of QS in the form of the synthesis of AHLs and Quinolone molecules with the aim to regulate an array of virulence-associated genes (Hodgkinson et al., 2012). Therefore, it is believed that SeNPs can disrupt AHL and quinolone-based QS mechanisms, thereby

reducing virulence in *P. aeruginosa*. This makes SeNPs a promising candidate for novel therapeutic agents that can effectively combat QS-controlled infections. Consequently, we conducted computational exploratory research into the QS-controlled functioning of SeNPs.

In *P. aeruginosa*, the production of 3-oxo-C12-HSL and C4-HSL is controlled by LasI and RhlI synthases, respectively. These signaling molecules then activate the transcriptional activators LasR and RhlR, resulting in the induction of genes responsible for virulence. In the absence or inactivation of LasR, the MvfR transcriptional regulator, the receptor of the PQS QS signal, regulates the RhlI expression and LasR-controlled LasI genes that activate the RhlI/R system and direct biological signal transduction to virulence gene expression toward QS activity (Moradali et al., 2017). Thus, SeNPs were targeted against the Las signaling system, Rhl signaling cascade along with PQS signaling machinery. To gain insights into the inhibitory mechanisms of SeNPs against AHL synthases (LasI/RhlI) and transcriptional regulatory receptor proteins (LasR/RhlR and MvfR), the current study conducted molecular docking analyses to predict the potential interacting positions of SeNPs on these proteins.

Consequently, we extracted the 3D crystal structures from the PDB database using the PDB IDs of 1RO5, 2UV0, and 4JVC, respectively, of the LasI synthase (Figure 1A), the transcriptional activator protein LasR (Figure 2A), and the MvfR transcriptional protein (Figure 9A). However, since no 3D crystal structure was available for the RhlI synthase and its regulatory protein in the PDB, we utilized the homology modeling method using the Robetta server to generate the 3D structure of the RhlI synthase (Figure 3A) and RhlR (Figure 4A). Homology modeling is a widely used technique for comparative modeling of protein structures when the PDB database lacks complete crystal structures. This is especially useful as protein sequences were generally more conserved than DNA sequences. Once a model protein has been generated, various structure validation programs are available to assess its geometrical conformations and stereochemical quality. Calculations for the Ramachandran plot were carried out with the help of the programs, such as PROCHECK, ERRAT, VERIFY-3D, and WHAT IF servers, followed by the SAVES server (Table 1).

Model validation of the RhlI synthase and RhlR conformation was performed using the phi ( $\Phi$ ) and psi ( $\Psi$ ) score analyses in a Ramachandran plot (Hollingsworth and Karplus, 2010). The modeled structure prediction depends on the highest sequence identity and coverage of the target sequence with the available template for model building. In the current study, the Ramachandran plot of the modeled RhlI synthase (Figure 3B) revealed that the number of non-glycine and non-proline residues is 177. Out of this, 157 (88.7%) were in the most favored regions along with 20 residues (11.3%) in the allowed regions and none in the outlier region. The allotment of main-chain torsion angle phi and psi evidently illustrated that the bulk of the amino acids are in a phi–psi distribution more or less reliable with right-handed alpha helices. These results imply that the stereochemical properties and quality of the model structure of the RhlI protein are quite suitable. Although previous studies (Laskowski et al., 1993) suggested that a good-quality model is expected to have a score over 90%, recent research (Williams and Cloete, 2022) demonstrated that the modeled structure is reliable

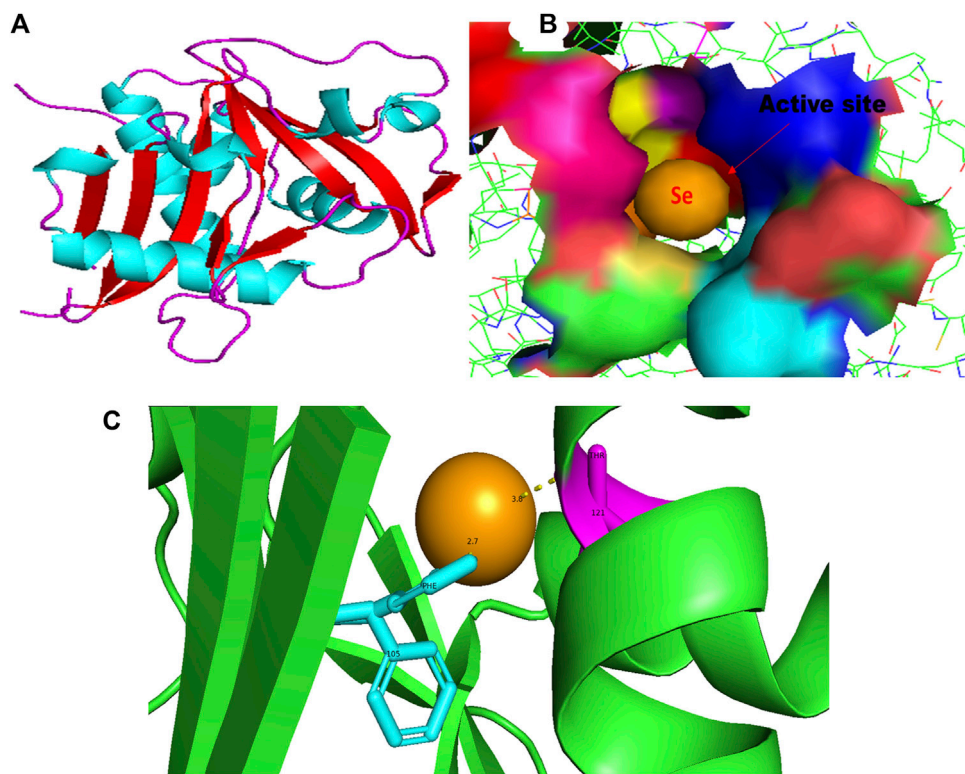


**FIGURE 1**

PyMol viewer showed the active location of PatchDock interactions of SeNPs with LasI. **(A)** 3D structure of AHL synthase LasI; **(B)** a close-up of the attachment of SeNPs to the LasI's catalytic site, with bound Se depicted as a sphere; and **(C)** LasI amino acid residues (Phe105 and Thr121) that interact with SeNPs.

if >80% of the residues are in the most favored region, followed by additional allowed regions for further residues (Williams and Cloete, 2022). This is very much in support of our model quality. In addition, if the model contains none of the residues in a disallowed region with the aforementioned conditions, then it is considered as a good-quality model. Scientific studies which report that a good-quality model having less than 90% in the most favored region are also available (Han et al., 2019; Chen et al., 2022; Williams and Cloete, 2022). Likewise, for RhIR, the Ramachandran plot revealed that 95.8% of the residues were in the preferred region, with 4.2% in the allowed region and none in the aberrant region (Figure 4B). The modeled tertiary structures of RhII synthase and RhIR were subjected to investigate the stability of the modeled proteins. For determining the stability of a protein and its complexes, analysis of molecular dynamics simulations is indispensable. So, a molecular dynamics simulation for 100 ns was carried out using GROMACS 2019 and the GROMOS 54a7 force field.

RMSD and RMSF were computed applying GRACE software for both the proteins RhII and RhIR to understand their stability levels and the degree of flexibility over the amino acid residues in order to understand homology model trajectories generated at 100 ns (Figures 3C, D; Figures 4C, D). Our experimental settings demonstrated the protein's stability over a brief period of time. The RMSD and RMSF calculations were evaluated and found to be under the threshold limit. The majority of amino acid residues in

both proteins had lesser RMSF profiles, which may account for the inflexibility of the proteins (Figures 5, 6). Despite certain deviations observed in the result, the RMSF values of these residues in RhII and RhIR stayed below 4.0 Å and 6.0 Å, respectively, Figures 3D, 4D. The RMSD values for the RhII and RhIR proteins were around 3.8 Å and 5.8 Å, respectively, as shown in Figure 3C and Figure 4C.

Pre- and post-molecular dynamics simulation structure superimpositions have been performed using PyMol. The final snapshot from the trajectory of molecular dynamics at 100ns was superimposed over the modeled protein of 0 ns (Figures 3E, F; Figures 4E, F), and it revealed that the post-molecular dynamics simulated structure (100 ns) was more stable and had the same characteristics as the modeled structure (0 ns). As depicted in Figure 3F and Figure 4F, this stability of the protein can be attributed to the various residues and interactions present on its side chain. Notably, there was only a slight fluctuation observed in the side chain, and a small flexible region was identified. This may be due to a lack of contact or the presence of flexible loops.

The use of molecular docking, a powerful computational approach, has been employed to model the atomic-level interactions between small molecules and proteins to elucidate their behavior within binding sites. The functional grooves or pockets responsible for identifying the protein's function are referred to as "active sites." Although the active site typically constitutes only 10%–20% of the total protein, it catalyzes the entire enzymatic reaction. As a result, identifying a protein's

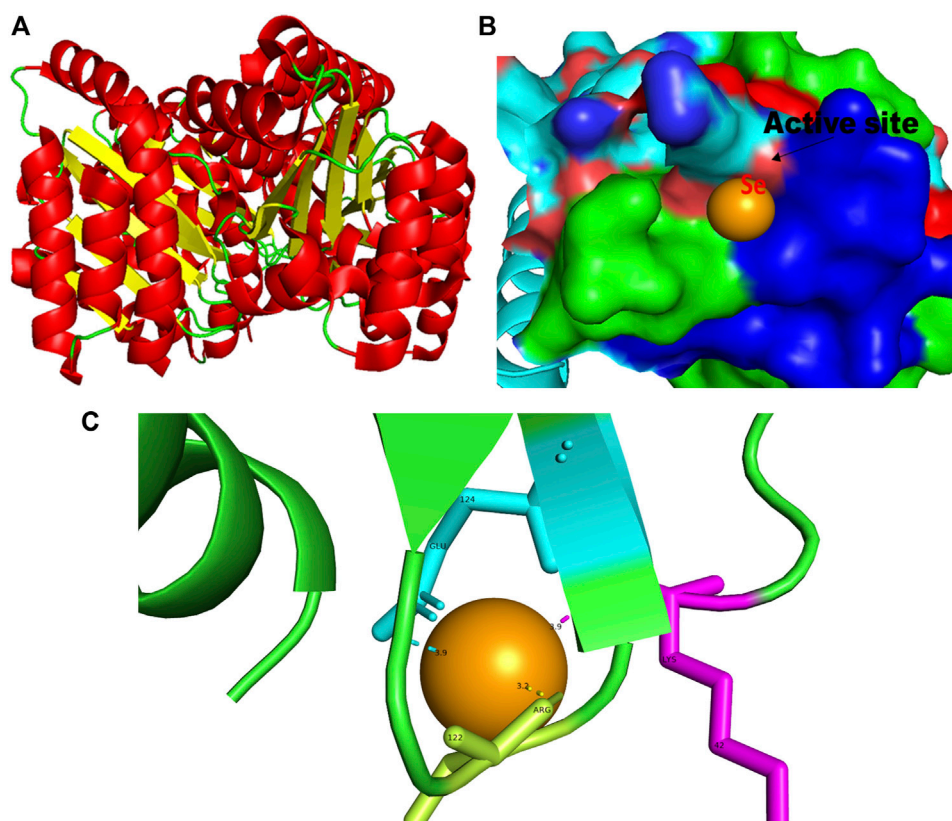


**FIGURE 2**

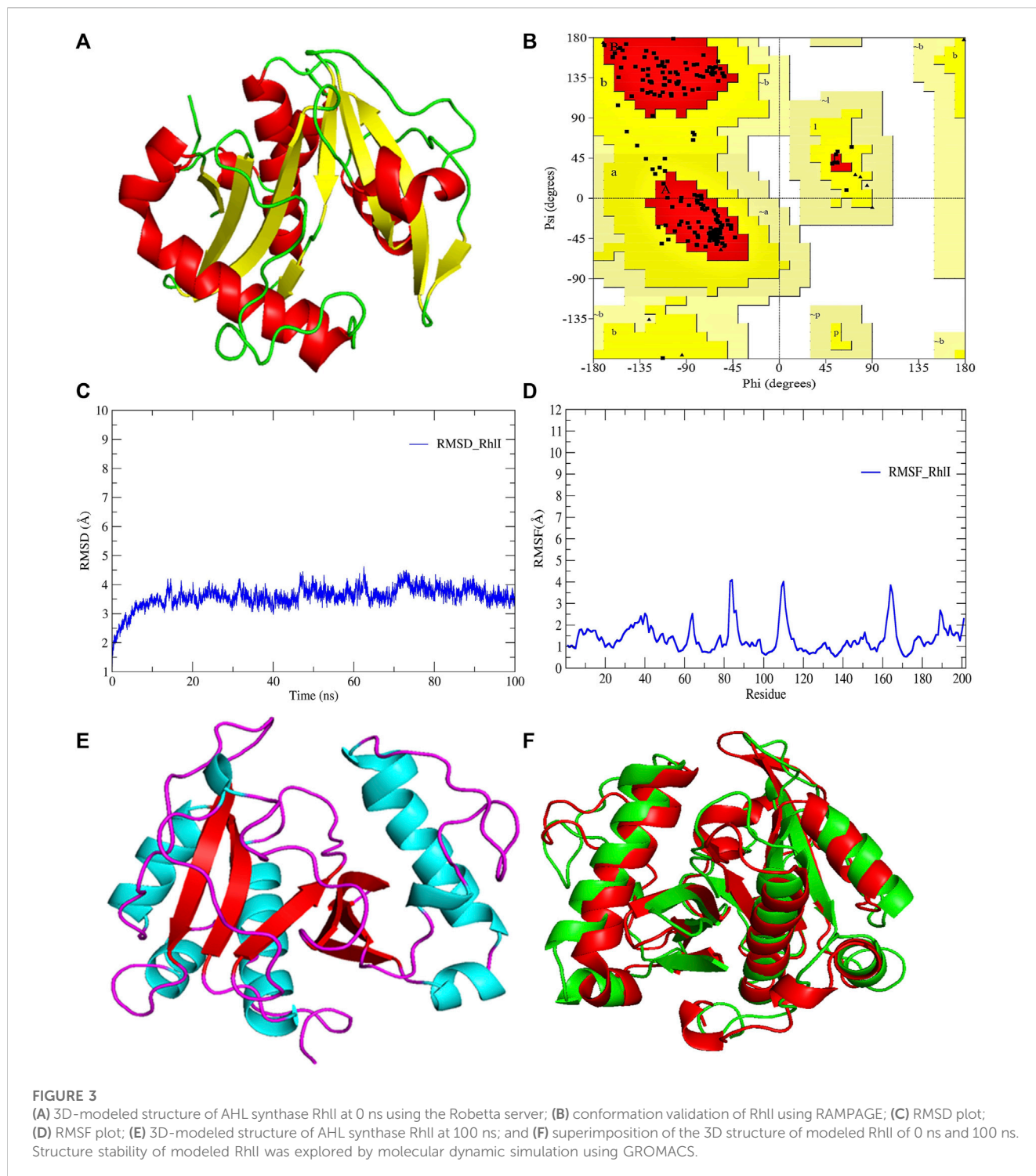
PyMol viewer showed the active location of PatchDock interactions of SeNPs with LasR. **(A)** 3D structure of transcriptional activator protein LasR; **(B)** a close-up of the attachment of SeNPs to LasR's catalytic site, with bound Se depicted as a sphere; and **(C)** LasR amino acid residues (Lys42, Arg122, and Glu124) that interact with SeNPs.

active or binding site is critical for understanding its functional behaviors. Hence, the targeted QS molecule docking/active site prediction was performed using CASTp (Table 2) for molecular docking studies.

In this study, using a PatchDock-based molecular docking approach, it was found that SeNPs were successfully docked into the AHL synthases LasI (Figure 1B) and RhII (Figure 7B), as well as the regulatory activator proteins LasR (Figure 2B) and RhIR (Figure 8B), and the transcriptional protein MvfR (Figure 9B). The docked structures after docking between the ligand and the respective interacting residues of QS proteins were displayed here using PyMol. On the basis of these docking positions, we speculated that SeNPs became 'locked' into the active site of specific proteins by their surrounding amino acid residues (Figures 1C, 2C, 7C, 8C, 9C). Table 3 displays the QS regulator proteins' docking geometric score, atomic contact energy (desolvation energy), and ligand-interacting residues. There have been reports in the past showing the effectiveness of SeNPs as anti-QS and anti-biofilm agents against various pathogenic bacteria. However, there was a lack of *in silico* understanding on the interaction with bacterial QS regulator proteins. Thus, in the present study, computational docking of SeNPs with QS proteins (LasI, LasR, RhII, RhIR, and MvfR) in the QS system of *P. aeruginosa* was performed.

### 3.1 LasI

An essential component of the QS system in *P. aeruginosa* is the monomeric signaling protein, LasI synthase, which regulates the activity of virulence factors in the respective bacteria. This protein shows interaction with SeNPs. According to the results of molecular docking examination, Se<sup>(0)</sup> binds to the catalytic residues phenylalanine and threonine of LasI synthase (Phe105-Se = 2.7 Å and Thr121-Se = 3.8 Å; Figure 1C). Therefore, the outcomes of a molecular docking of SeNPs with LasI determine that strong interactions and promising binding effectiveness at the active site of LasI have led to the formation of a more stable complex with a desolvation energy of  $-55.23 \text{ kcal mol}^{-1}$ . It displayed hydrogen bond interactions with Phe105 (2.7 Å) and Thr121 (3.8 Å) protein residues with a docking score of 808. In accordance with our study, the molecular interaction of nanoparticles has been reported in a few studies. Shah and their team also noted an electrostatic interaction of the Asp73 residue of LasI protein with silver nanoparticles (AgNPs) after docking analysis (Shah et al., 2019), which was similarly reported by Ali et al. (2017). Mishra and Mishra (2021) opined that copper nanoparticles (CuNPs) interact with amino acids Ser103, Leu102, Glu101, and Met79 in the LasI active site. Their study revealed that the formation of a stable protein–ligand complex of LasI and CuNP has a binding energy of  $-4.32 \text{ kcal mol}^{-1}$  (Mishra and Mishra, 2021). In the

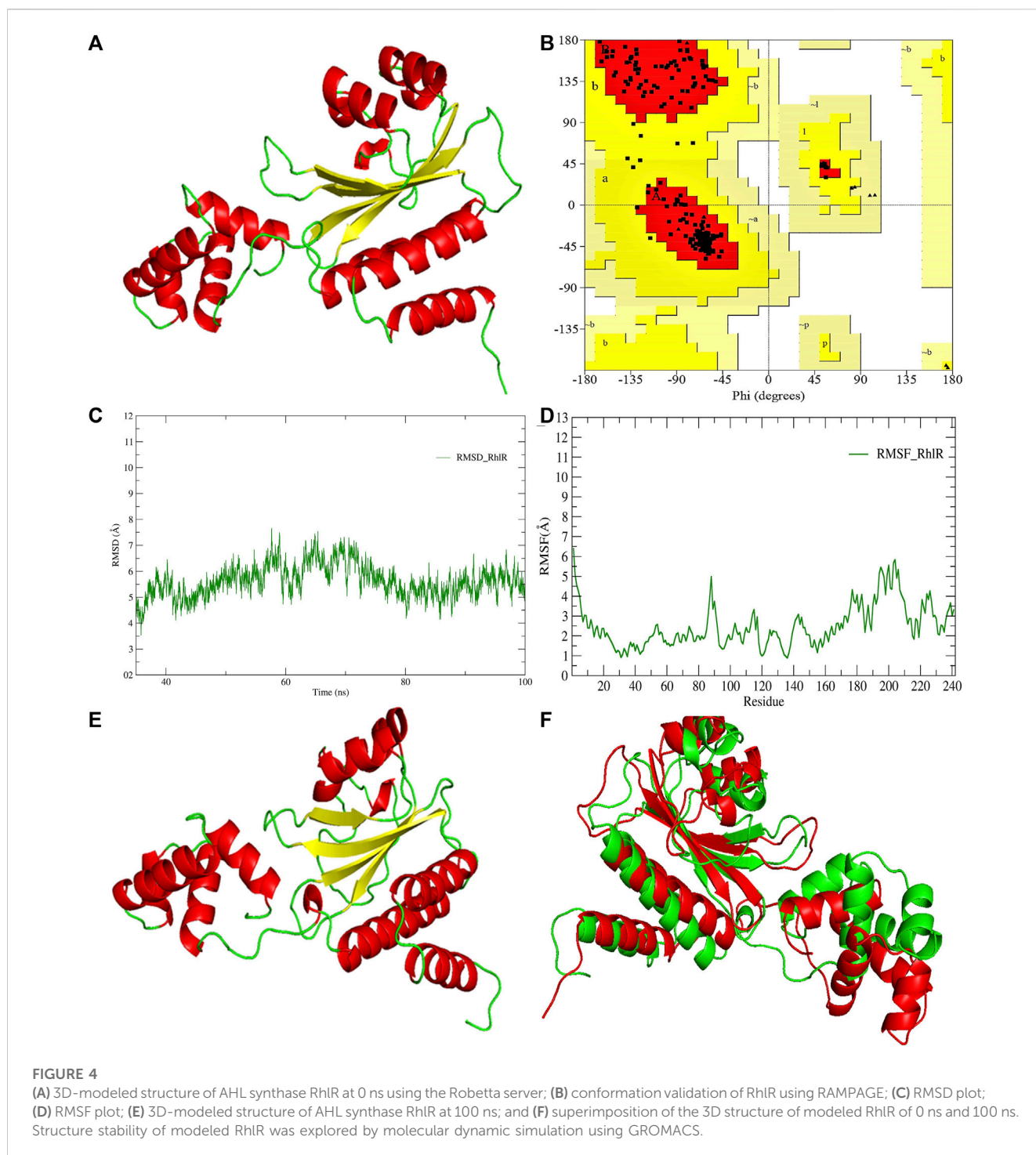


current study, molecular docking analysis demonstrated SeNPs' promising binding efficacy at the active site of LasI. The desolvation energy of the SeNP-LasI complex was notably higher ( $-55.23 \text{ kcal mol}^{-1}$ ) compared to the well-known QSI furanone C30 ( $-2.39 \text{ kcal mol}^{-1}$ ) and the natural ligand gingerol ( $-2.55 \text{ kcal mol}^{-1}$ ) mentioned in other scientific reports (Shah et al., 2019; Mishra and Mishra, 2021). This finding strongly suggested that SeNPs could potentially contribute to the inhibition of AHL production.

### 3.2 LasR

LasR (PDB ID: 2UV0) is a transcriptional activator protein that spans 175 amino acids. It functions by binding to the autoinducer produced by the Las synthase protein. As a transcriptional activator, LasR plays a crucial role in activating multiple genes associated with virulence (Bottomley et al., 2007). Notably, the Las system acts as the primary controller of QS and triggers the countenance of both Rhl

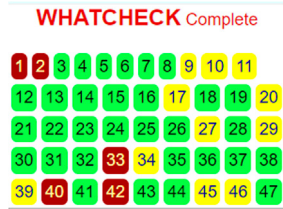
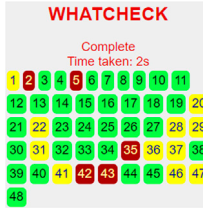




and Pqs signaling pathways in *P. aeruginosa* (Rathinam et al., 2017). Docking studies of SeNPs (Figure 2C) show a hydrogen bond interaction with arginine and a hydrophobic interaction with the amino acid lysine and glutamate residues of the LasR receptor (Arg122-Se = 3.2 Å, Lys42-Se = 3.9 Å, and Glu124-Se = 3.9 Å; Figure 2C) active site and make the bond with residues of the protein. The desolvation energy of the SeNPs was  $-54.3 \text{ kcal mol}^{-1}$  with a docked score of 632, demonstrating that SeNP and LasR have effective and stable binds. Shah and co-workers (2019) reported

AgNP production using the aqueous leaf extract of *Piper betle* and reported the electrostatic interaction with the amino acid Asp73 in the LasR active site (Shah et al., 2019), which was found to be in support of our study. A similar finding also has been reported by Vyshnava et al. (2016). In another report, it was stated that CuNP interacts with amino acid glutamic acid in the LasR active site displaying a significant binding energy  $-6.78 \text{ kcal mol}^{-1}$  (Mishra and Mishra, 2021). The desolvation energy of SeNP ( $-54.3 \text{ kcal mol}^{-1}$ ) was notably higher than the reported known QS inhibitor (QSI)

TABLE 1 Structural validation of modeled proteins.

PROTEIN	VERIFY 3D	ERRAT	WHATCHECK	RAMACHANDRAN PLOT																											
RhII	93.03% of the residues have averaged 3D-1D score $\geq 0.2$	Overall quality factor		<p>Plot statistics</p> <table border="1"> <tr> <td>Residues in most favoured regions [A,R,L]</td> <td>157</td> <td>88.7%</td> </tr> <tr> <td>Residues in additional allowed regions [G,S,L,P]</td> <td>20</td> <td>11.3%</td> </tr> <tr> <td>Residues in generously allowed regions [I,-,b,-l,-p]</td> <td>0</td> <td>0.0%</td> </tr> <tr> <td>Residues in disallowed regions</td> <td>0</td> <td>0.0%</td> </tr> <tr> <td>Number of non-glycine and non-proline residues</td> <td>177</td> <td>100.0%</td> </tr> <tr> <td>Number of end-residues (excl. Gly and Pro)</td> <td>2</td> <td></td> </tr> <tr> <td>Number of glycine residues (shown as triangles)</td> <td>11</td> <td></td> </tr> <tr> <td>Number of proline residues</td> <td>11</td> <td></td> </tr> <tr> <td>Total number of residues</td> <td>201</td> <td></td> </tr> </table> <p>Based on an analysis of 118 structures of resolution of at least 2.0 Angstroms and <math>R</math>-factor no greater than 20%, a good quality model would be expected to have over 90% in the most favoured regions.</p>	Residues in most favoured regions [A,R,L]	157	88.7%	Residues in additional allowed regions [G,S,L,P]	20	11.3%	Residues in generously allowed regions [I,-,b,-l,-p]	0	0.0%	Residues in disallowed regions	0	0.0%	Number of non-glycine and non-proline residues	177	100.0%	Number of end-residues (excl. Gly and Pro)	2		Number of glycine residues (shown as triangles)	11		Number of proline residues	11		Total number of residues	201	
	Residues in most favoured regions [A,R,L]	157			88.7%																										
Residues in additional allowed regions [G,S,L,P]	20	11.3%																													
Residues in generously allowed regions [I,-,b,-l,-p]	0	0.0%																													
Residues in disallowed regions	0	0.0%																													
Number of non-glycine and non-proline residues	177	100.0%																													
Number of end-residues (excl. Gly and Pro)	2																														
Number of glycine residues (shown as triangles)	11																														
Number of proline residues	11																														
Total number of residues	201																														
Pass	93.2292																														
RhIR	97.93% of the residues have averaged 3D-1D score $\geq 0.2$	Overall quality factor		<p>Plot statistics</p> <table border="1"> <tr> <td>Residues in most favoured regions [A,R,L]</td> <td>206</td> <td>95.8%</td> </tr> <tr> <td>Residues in additional allowed regions [G,S,L,P]</td> <td>9</td> <td>4.2%</td> </tr> <tr> <td>Residues in generously allowed regions [I,-,b,-l,-p]</td> <td>0</td> <td>0.0%</td> </tr> <tr> <td>Residues in disallowed regions</td> <td>0</td> <td>0.0%</td> </tr> <tr> <td>Number of non-glycine and non-proline residues</td> <td>215</td> <td>100.0%</td> </tr> <tr> <td>Number of end-residues (excl. Gly and Pro)</td> <td>2</td> <td></td> </tr> <tr> <td>Number of glycine residues (shown as triangles)</td> <td>14</td> <td></td> </tr> <tr> <td>Number of proline residues</td> <td>10</td> <td></td> </tr> <tr> <td>Total number of residues</td> <td>241</td> <td></td> </tr> </table> <p>Based on an analysis of 118 structures of resolution of at least 2.0 Angstroms and <math>R</math>-factor no greater than 20%, a good quality model would be expected to have over 90% in the most favoured regions.</p>	Residues in most favoured regions [A,R,L]	206	95.8%	Residues in additional allowed regions [G,S,L,P]	9	4.2%	Residues in generously allowed regions [I,-,b,-l,-p]	0	0.0%	Residues in disallowed regions	0	0.0%	Number of non-glycine and non-proline residues	215	100.0%	Number of end-residues (excl. Gly and Pro)	2		Number of glycine residues (shown as triangles)	14		Number of proline residues	10		Total number of residues	241	
	Residues in most favoured regions [A,R,L]	206			95.8%																										
Residues in additional allowed regions [G,S,L,P]	9	4.2%																													
Residues in generously allowed regions [I,-,b,-l,-p]	0	0.0%																													
Residues in disallowed regions	0	0.0%																													
Number of non-glycine and non-proline residues	215	100.0%																													
Number of end-residues (excl. Gly and Pro)	2																														
Number of glycine residues (shown as triangles)	14																														
Number of proline residues	10																														
Total number of residues	241																														
Pass	95.279																														

furanone C30 ( $-5.44 \text{ kcal mol}^{-1}$ ) (Shah et al., 2019), suggesting effective and steady interactions of SeNP and LasR. Therefore, this discovery indicated that the silencing of the transcriptional regulator LasR activity can be ascribed to the anti-QS activity of SeNPs along with their anti-biofilm function.

### 3.3 RhII

The RhII synthase is responsible for the production of N-butyryl-L-homoserine lactone, also known as C4-HSL. When C4-HSL binds to its cellular receptor RhIR, the virulence genes in *P. aeruginosa* are activated (Rutherford and Bassler, 2012). As a result of PatchDock, SeNP shows appreciable atomic contact energy (desolvation energy),  $-56.53 \text{ kcal mol}^{-1}$ , and a binding score of 712 with the protein residues, leucine and valine, in the active site of the RhII synthase (Leu102-Se = 3.7 Å and Val138-Se = 3.2 Å; Figure 7C). In support of our study, Mishra and co-workers (2021) stipulated the similar interaction between known QS inhibitor gingerol and the amino acid Leu102 and Val138 of RhII-binding pocket with binding energy  $-4.19 \text{ kcal mol}^{-1}$  (Mishra and Mishra, 2021). Likewise, they also reported that CuNP interacted with amino acid glutamic acid and forms strong complex with RhII with binding energy  $-4.43 \text{ kcal mol}^{-1}$ . These findings suggested that SeNP bonded strongly with RhII. These results indicated that the suppression of transcriptional regulator RhII endorsed the anti-QS activity of SeNPs.

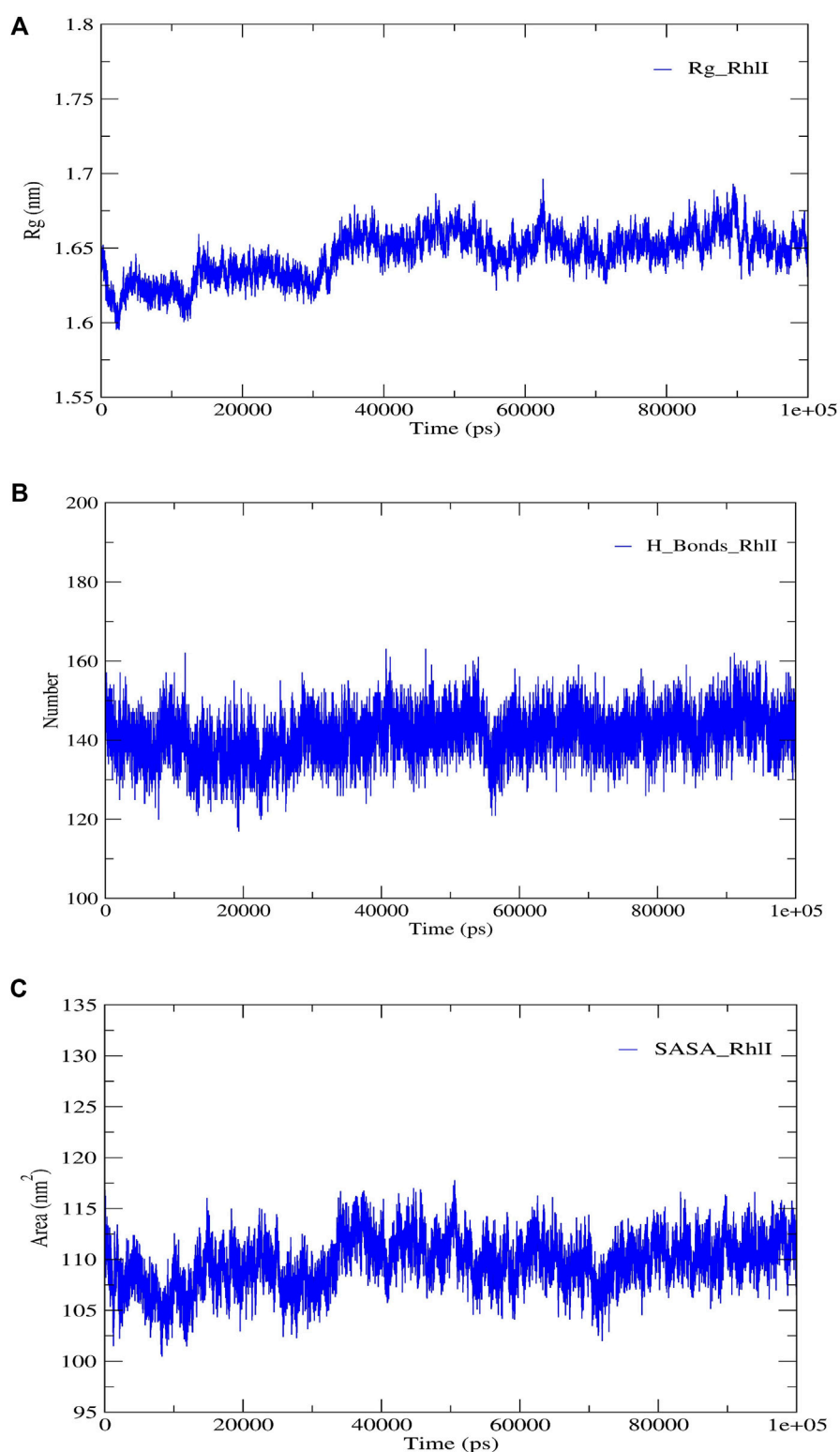
### 3.4 RhIR

RhIR functions as a cellular receptor for AHL synthesized by the RhII synthase, activating genes essential for virulence. The protein RhIR shows good binding with atomic contact energy  $-75.28 \text{ kcal mol}^{-1}$  and a binding score (720) with SeNPs. SeNPs display hydrogen bond interactions with tyrosine and histidine residues of the RhIR receptor active site (Tyr43-Se = 2.9 Å, Tyr45-Se = 3.4 Å, and His61-Se = 3.5 Å; Figure 8C). This finding suggested that SeNP bonded

strongly with RhIR. These results indicated that the suppression of transcriptional regulator RhIR endorsed the anti-QS activity of SeNPs. Mishra and team stipulated the interaction between the known QS inhibitor gingerol and the amino acids Phe, Arg, Ser, Val, and Ile of the RhIR-binding pocket with binding energy  $-1.82 \text{ kcal mol}^{-1}$ . The gingerol-interacting residues are in the active site line predicted in the current study. Likewise, they reported that CuNP interacts with amino acid glutamic acid and forms a strong complex with RhII with binding energy  $-4.44 \text{ kcal mol}^{-1}$  (Mishra and Mishra, 2021).

### 3.5 MvfR

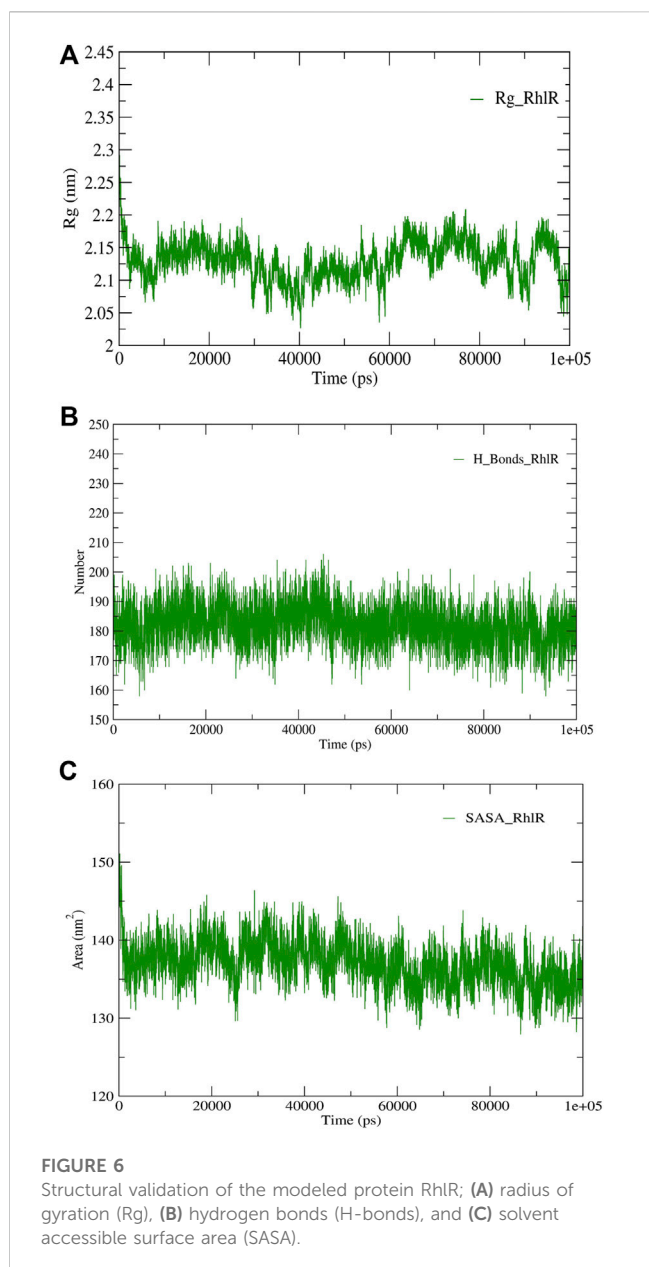
In addition to LasI/LasR, PQS (*Pseudomonas* quinolone signal) is an additional QS system in *P. aeruginosa* that plays a significant role in biofilm formation (Dubern and Diggle, 2008). The synthesis of PQS molecules is controlled by the pqsABCDE operon through a transcriptional regulator protein called MvfR (PqsR). This protein also regulates the secretion of pyocyanin and rhamnolipid, as well as the growth of biofilm. Thus, targeting the inhibition of PQS is considered a promising strategy for attenuating pathogenic bacteria, particularly in biofilm-related infections (Rampioni et al., 2016; Parai et al., 2018). The PatchDock result shows SeNPs' interaction with MvfR and forms the hydrogen bond with leucine and a hydrophobic interaction with arginine residues of the MvfR transcriptional protein (Leu208-Se = 3.2 Å and Arg209-Se = 4.0 Å; Figure 9C). The active site residues of MvfR exhibited a stable interaction with SeNPs, displaying a higher desolvation energy ( $-65.03 \text{ kcal mol}^{-1}$ ) compared to QSI furanone C30 ( $-41.57 \text{ kcal mol}^{-1}$ ), with a binding score of 724 (Table 3). This result is in line with a previous investigation (Parai et al., 2018) that demonstrated stable integration of reserpine into the binding pocket of MvfR. Gómez-Gómez et al. (2019) and Shah et al. (2019) reported that the docking study of the AgNP with MvfR showed acceptor interaction with Asn206, Leu207, and Arg209, which advocated the interaction of SeNP and MvfR in the current study. To summarize, the computational analysis revealed that SeNPs established favorable interactions with mvfR, potentially suppressing

**FIGURE 5**

Structural validation of the modeled protein RhlI; (A) radius of gyration (Rg), (B) hydrogen bonds (H-bonds), and (C) solvent accessible surface area (SASA).

the PQS signaling in *P. aeruginosa* infections. Consequently, SeNPs hold promise as potential agents for combating drug-resistant biofilm formation associated with *P. aeruginosa*. The current molecular-

docking investigations (Figures 1, 2; Figures 7–9) reveal unequivocally that selenium strongly locks within the catalytic groove of the active domain of the AHL synthase (LasI/RhlI) and



receptor proteins (LasR/RhlR), thereby inhibiting the expression and signaling of QS-controlled virulence genes and halting the formation of biofilm in *P. aeruginosa*.

The established mechanism of action of SeNPs is not reported (Singh et al., 2017; Gómez-Gómez et al., 2019; Shah et al., 2019) and is warranted to be defined by *in vitro* and *in vivo* experiments. In addition, SeNPs does not bear chemical structural similarity to AHLs and SAM counterparts in QS-regulated biofilm formation, suggesting a novel approach to inhibiting QS-controlled genes and a possible treatment option for *P. aeruginosa*. A conclusive statement about their mechanism of action may be currently available in the present study. However, the mode of action for other nanoparticles have been hypothesized and presented by other scientists (Yin et al., 2020). For instance, AgNPs are effective antimicrobial agents that produce silver ions responsible for the inhibition of bacterial enzymatic systems including DNA synthesis (Wang et al., 2018). Many mechanisms have been postulated to underlie silver antimicrobial action, including cell wall and cytoplasmic membrane disruption, inhibition of protein synthesis machinery by denaturation of ribosomes, interference with ATP production and chemosmosis, production of ROS, and interference with DNA replication machinery (Yin et al., 2020). Therefore, on the basis of the hypothesis about the mechanism of action of AgNPs, we foresee that SeNPs can serve as potential monotherapeutic agents or conjugates with available drugs, in order to enhance their efficacy and biocompatibility with reduced toxicity. In the current study, we examined the potential of SeNPs. Selenium is an essential nutrient, used for dietary consumption required for human metabolism. Thus, it is safe for use at nanoscale (Gunti et al., 2019). In addition, smaller size and high volume-surface area make the nanoparticles enhanced substitutes to increase the penetration to microbial cells for action and also to develop a drug delivery system (Singh et al., 2017).

Two researchers suggested that glutamine, histidine, serine, threonine, and tyrosine significantly enhanced growth and biofilm formation (Velmourougane and Prasanna, 2017). Other studies also suggested that asparagine, histidine, leucine, methionine, tryptophan, and tyrosine are involved in the architecture of biofilm assembly (Kolodkin-Gal et al., 2010). Our findings showed interactions of SeNPs with key amino acids residues, such as glutamine, histidine, threonine, and tyrosine (Table 3), in ligand binding or active domains of the QS signaling proteins. Moreover, selenium (Se) is more reactive towards electrophiles due to their lower electronegativity and nucleophilic behavior; thus, it is a hydrogen (H) bond acceptor (Goldsztejn et al., 2022) that supports our data (Table 3). In addition, the PDB survey also suggested the occurrence of strong Se-H bonding.

**TABLE 2** Active-binding sites of QS proteins.

Protein name	Amino acid positions in the active site
LasI	Val (26, 143, 148), <b>Phe</b> (27, 84, 105, 117), Arg (30, 104), Trp (33, 69), Met (79), Glu (106), Leu (102), Ser (103), Ala (106), Ile (107), and <b>Thr</b> (121, 144, 145)
LasR	<b>Phe</b> (07, 167), Leu (08, 10, 125, 159, 165), <b>Glu</b> (11, 124, 168), <b>Arg</b> (12, 122), Ser (13, 14, 44, 161), Gly (15, 120, 123, 164), Trp (19), Pro (41), <b>Lys</b> (42), Asp (43), His (119), Ala (121, 163), and Gln (160)
RhlI	<b>Val</b> (27, 135, 138, 163), Phe (28, 120, 173), <b>Leu</b> (32, 80, 81, 88, 102, 124, 168), Trp (34), Glu (101, 166), Ser (103, 123), Arg (104), Tyr (105), Ala (107, 109, 110, 137), Asp (111), Thr (139, 140), Gln (161), Lys (164), and Gly (165)
RhlR	Gln (25), Phe (28), Ala (29, 44), Glu (32), <b>Tyr</b> (43, 45), <b>His</b> (61), Gly (62), and Thr (63)
MvfR	Ala (102, 168, 237), Pro (129, 210, 238), Ile (149, 186, 189, 195, 236, 263), Thr (166, 265), Lys (167), Val (170, 211), Gly (194), Ser (196, 255), <b>Leu</b> (197, 207, 208, 254), Asn (206), <b>Arg</b> (209), Phe (221), Met (224), Trp (234), and Tyr (258)

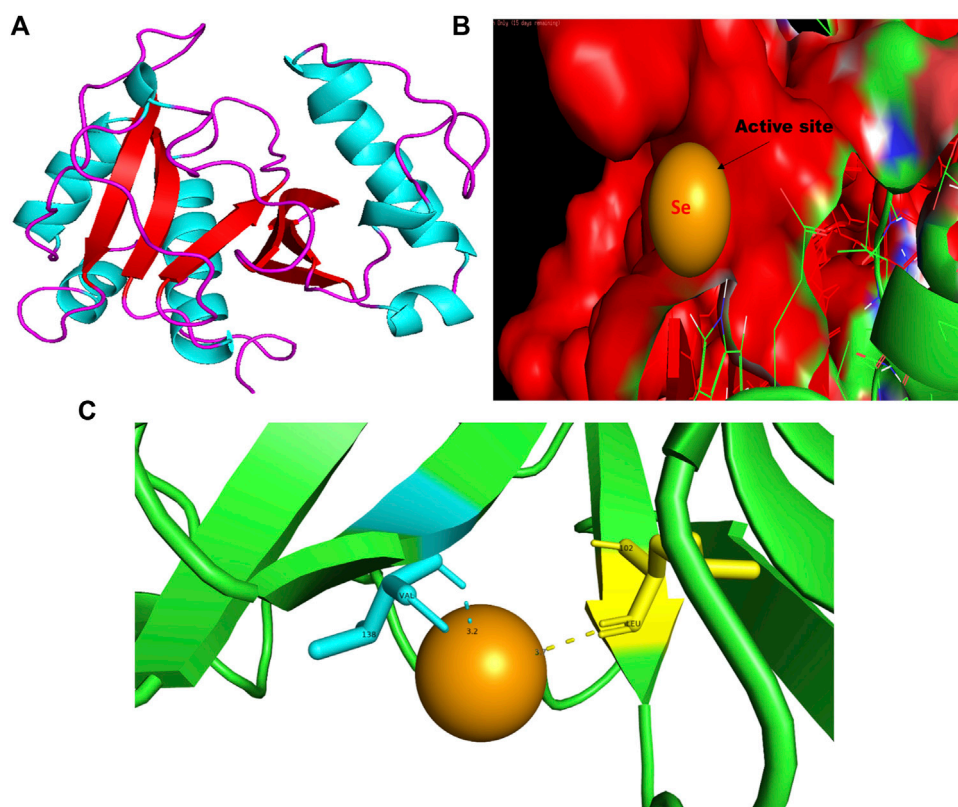


**FIGURE 7**

PyMol viewer showed the active location of PatchDock interactions of SeNPs with RhlI. (A) 3D-modeled structure of AHL synthase RhlI at 100 ns using the Robetta server; (B) a close-up of the attachment of SeNPs to RhlI's catalytic site, with bound Se depicted as a sphere; and (C) RhlI amino acid residues (Leu102 and Val138) that interact with SeNPs.

The active site residues of examined proteins (Table 2) are involved in the interaction with SeNPs, where amino acid residues show strong hydrogen and hydrophobic bond formation desolvation energy or atomic contact energy or binding energy ( $\text{kcal mol}^{-1}$ ) represented in Table 3. Generally, these binding energies reflect the mirror of Gibbs-free energy, which describe the efficiency of any reaction as well as binding or interaction of the residues. Negative value (–) of binding energy represents higher affinity of the residues resulting in strong interactions. To the best of our knowledge, unavailability of the co-ordinate or geometric confirmation file of SeNPs to support any available force field narrowed down the possibilities to perform post-docking simulation for further energy calculations.

In the present study, our analysis reveals the potential of SeNPs that can be used as an anti-QS agent monotherapeutically or as a conjugate with available therapeutics to increase efficacy. We examined the active binding sites (Table 2) of the targeted protein, and all the interactions in the present study revealed that SeNPs could bind at the active domain of the examined protein.

LasI is the counterpart of the AHL synthase. Biochemical studies, both *in vitro* and *in vivo*, demonstrated that enzymes in the LuxI family (for example, LasI) used S-adenosyl-methionine (SAM) and Acyl-acyl-carrier protein (Acyl-ACP) as a substrate to produce AHL molecules which stimulate the QS towards biofilm formation as well as adaptive mode of drug resistance. In the current

study, SeNPs interacts with LasI residues, Phe105, which belongs to the counterpart residues of the AHL synthase, and Thr121 which is a binding site of SAM with AHL synthase to generate a signal and produce AHL molecules (Gould et al., 2004; Lidor et al., 2015; Maisuria et al., 2016). Therefore, these findings lead to an understanding that SeNPs can also competitively bind with SAM and AHL synthase active sites to suppress the stimulus of QS signals (Figure 10; Table 3). The LasI synthase receptor protein, LasR, has two functional domains, namely, 1) ligand-binding domain (LBD) and 2) DNA-binding domain. Zou and Nair (2009) established that the LBD of LasR contains an L3 loop (active binding pocket) with residue length Leu40 to Phe51 (Zou and Nair, 2009). In addition, Paczkowski and coworkers (2019) demonstrated that the LasR binding pocket (Leu40-Phe51) displays significant flexibility in accommodating different ligands (Paczkowski et al., 2019). Therefore, in our study, SeNPs are known to interact with Lys42 of the LasR-LBD (L3 loop) through hydrophobic interaction and advocate the inhibitory potential of SeNPs against AHL production to stop QS in *P. aeruginosa* (Figure 10). A research group showed that the LBD of RhlI is made up of an activation, allosteric, and inhibition pocket including Leu102 and V138 and explained as a potential target to design an antagonist molecule (Shin et al., 2019), which supports our study (Table 3). Similarly, Simanek and team (2022) demonstrated that pycocyanin production, a virulence factor of biofilm, is controlled through

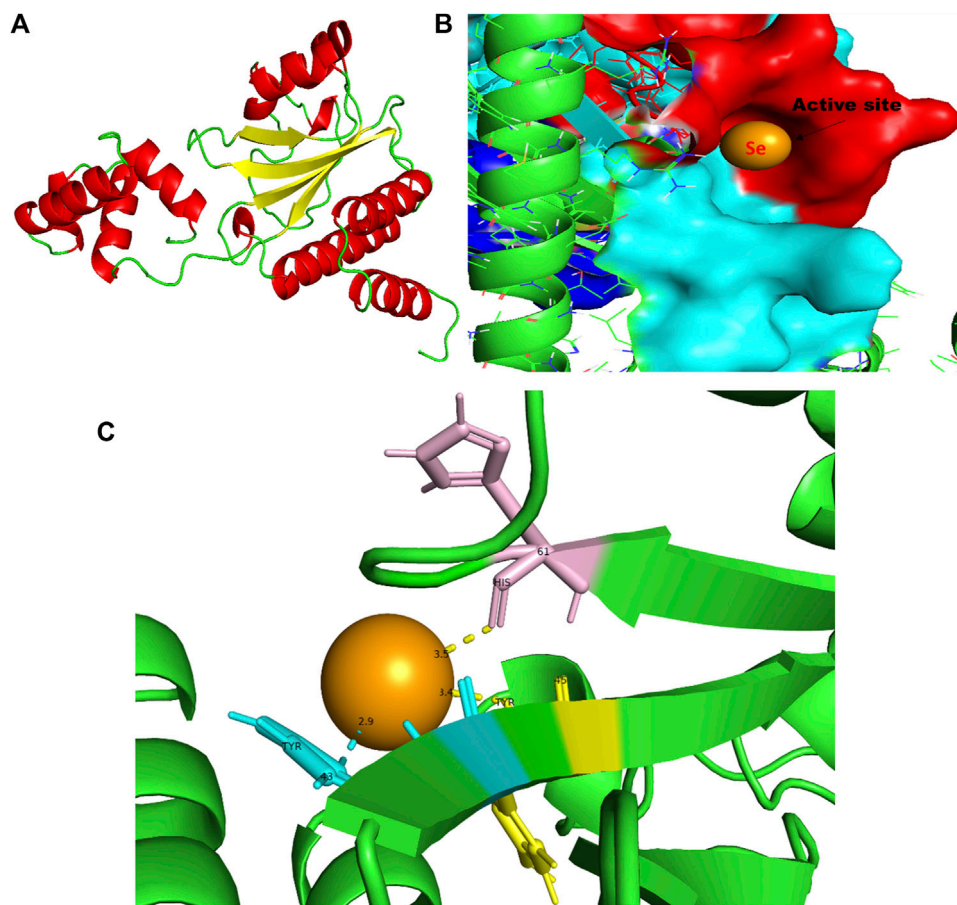


**FIGURE 8**

PyMol viewer showed the active location of PatchDock interactions of SeNPs with RhIR. (A) 3D modeled structure of AHL synthase RhIR at 100 ns using the Robetta server; (B) a close-up of the attachment of SeNPs to the RhIR's catalytic site, with bound Se depicted as a sphere; (C) RhIR amino acid residues (Tyr43, Tyr45, and His61) that interact with SeNPs.

physical interaction between RhIR and PQSE, the last gene in the operon of PQS synthesis (Simanek et al., 2022). Another research study showed the straight involvement of PQS in rhamnolipid synthesis (Reis et al., 2011). Moreover, a team of researchers (Ilangovan et al., 2013) showed the functional ligand-binding domain of MvfR containing a hydrophobic pocket with residues of Leu208 and Arg209. Our results corroborate with the previously published literature (Ilangovan et al., 2013) and found that SeNPs interacted with Leu208 (hydrogen bond) and Arg209 (hydrophobic bond) and justify its inhibitory capacity to obstruct the PQS molecules resulting in the inactivation of the RhII/R QS system (Figure 10). Overall, our finding points towards the understanding that particular protein residues are strongly bonded with SeNPs and can act potentially toward imparting the transcriptional signals resulting in the suppression of virulence factors and downregulation of biofilm formation.

Moreover, we show for the initial moment that SeNPs can attach to the signal synthases LasI (Figure 1) and RhII (Figure 7), despite the fact that their interaction and binding have not previously been documented in the literature. We proposed several possible strategies by which SeNPs disrupt QS networks based on our *in*

*silico* assessments as follows: 1) Inhibition of S-adenosyl methionine (SAM) biosynthesis: SAM functions as an amino donor in the synthesis of the homoserine lactone ring moiety. The manufacture of SAM must be inhibited in order to stop AHL formation. It has been speculated that SeNPs attach to SAM, depleting SAM levels and preventing the production of AHL (Figure 10). 2) Inhibition of LasI/RhII synthase: Inhibition of signal biosynthesis (LasI/RhII synthase) can be achieved through SeNPs binding to AHL synthase, ultimately hindering the enzymatic activity. Consequently, if AHL production ceases, QS will not occur, as illustrated in Figure 10. 3) Signal receptor proteins LasR and RhIR can be interfered with: Once the bacterial cell density reaches a specific threshold, the LasI/R QS system is triggered. Se binds to LasR's active site, forming the Se-LasR complex, which then suppresses RhII expression as well as LasR-controlled genes, including LasI signal synthase. As a result, the RhII/R system is deactivated, leading to the inhibition of QS-controlled virulence genes expression, as shown in Figure 10. 4) Interference with *Pseudomonas* quinolone signaling proteins MvfR: Se binds to MvfR's active site, resulting in the Se-MvfR complex, which suppresses MvfR and RhIR controlled gene expression, leading to

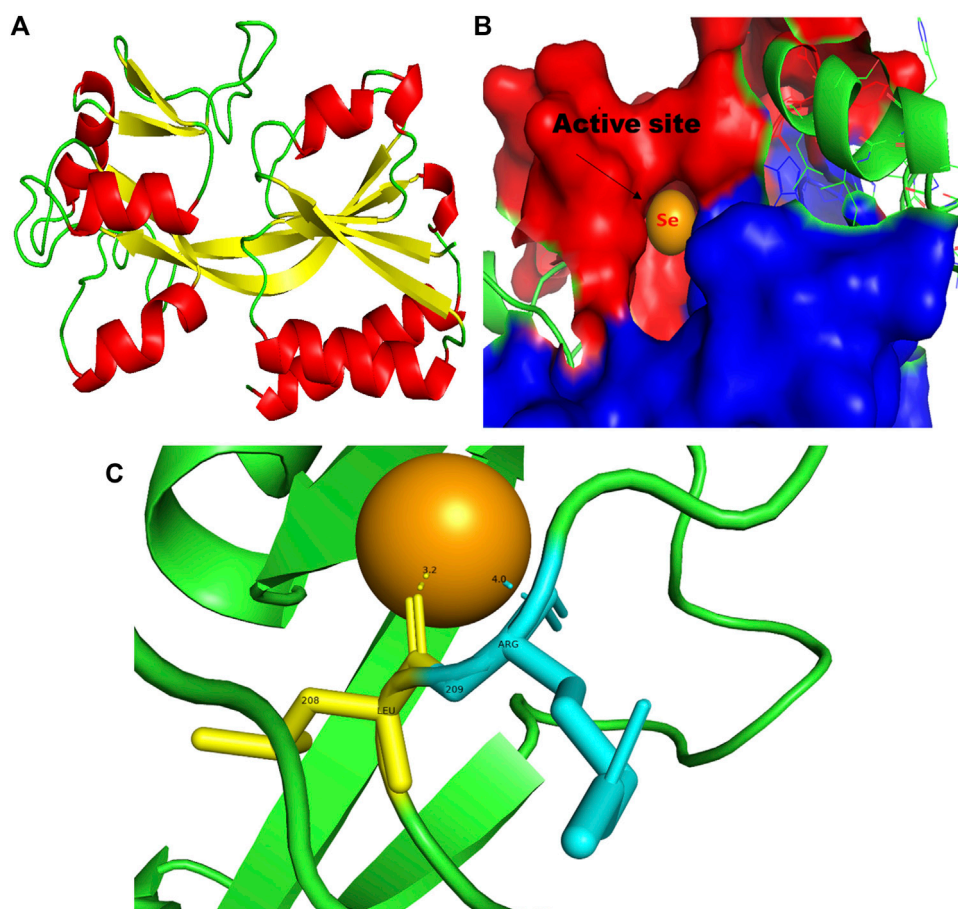
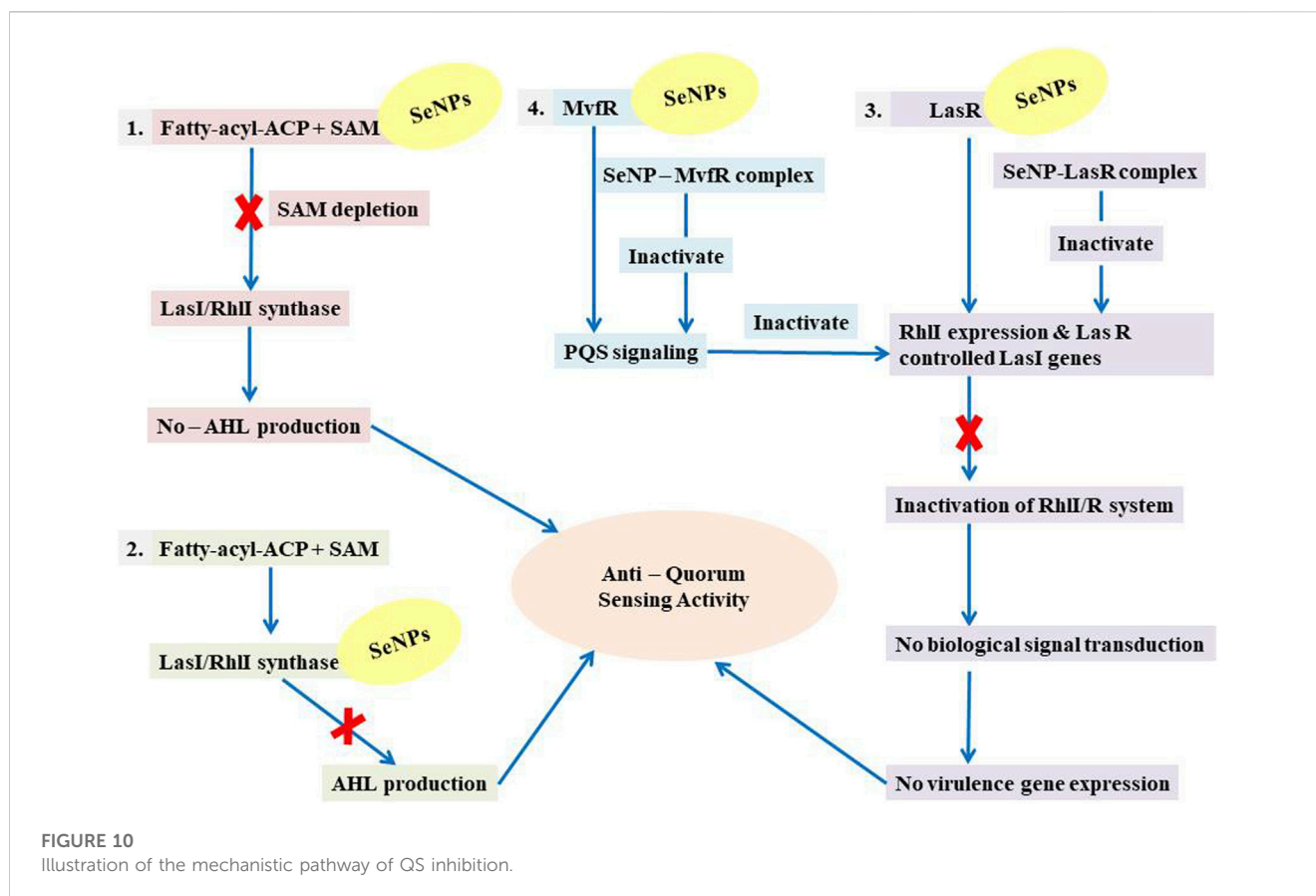


**FIGURE 9**

PyMol viewer showed the active location of PatchDock interactions of SeNPs with MvfR. **(A)** 3D structure of the transcription regulatory protein MvfR; **(B)** a close-up of the attachment of SeNPs to the MvfR's catalytic site, with bound Se depicted as a sphere; and **(C)** MvfR amino acid residues (Leu208 and Arg209) that interact with SeNPs.

**TABLE 3** Docking result of the inhibitory potential of SeNPs with QS proteins.

Protein	Ligand	Binding score	Area	Atomic contact energy (kcal mol <sup>-1</sup> )	Name of interacting amino acids at active sites of proteins	
					Amino acid residues	Bond length (Å)
LasI	SeNPs	808	95.30	-55.23	Phe (105)	2.7
					Thr (121)	3.8
LasR	SeNPs	632	71.50	-54.30	Lys (42)	3.9
					Arg (122)	3.2
					Glu (124)	3.9
RhII	SeNPs	712	87.50	-56.53	Leu (102)	3.7
					Val (138)	3.2
RhIR	SeNPs	720	77.90	-75.28	Tyr (43)	2.9
					Tyr (45)	3.4
					His (61)	3.5
MvfR	SeNPs	724	79.80	-65.03	Leu (208)	3.2
					Arg (209)	4.0



the deactivation of the MvfR/RhlR system. Consequently, the transcription of QS-regulated virulence genes is blocked and inhibited, as depicted in Figure 10. This study reveals the inhibitory potential of SeNPs using multiple bioinformatics tools. As a result, they may facilitate the development and implementation of such compounds to increase anti-quorum sensing reactions during *P. aeruginosa* infection.

## 4 Conclusion

The link between QS and bacterial pathogenicity is almost universally acknowledged. Interference bacterial cell-to-cell communication has been determined to be a promising technique for developing novel antimicrobial, anti-QS, and chemotherapeutic drugs. This opens the way for new antivirulence chemicals to be developed that are both effective and efficient. Inhibition of QS has the potential to reduce virulence. A similar conclusion was found about the anti-QS activity of selenium nanoparticles using computational investigation in the present study. The docking results demonstrated that SeNPs bind to the active sites of LasI/R, RhlI/R, and MvfR with consistent binding energies, suggesting that they could be used as an antivirulence agent against *P. aeruginosa* QS signaling in the future. Surprisingly, selenium nanoparticles bear no chemical structural similarities to AHL

counterparts, suggesting a novel approach to inhibiting QS-controlled genes and a possible treatment option for *P. aeruginosa* infections. The interaction of selenium nanoparticles with the AHL synthase (LasI/RhII) may interfere with the production of AHL, which may impede QS signaling. By attaching to receptor proteins (LasR/RhlR and MvfR), they also promise to suppress transcriptional activator activity. The molecular docking investigation found that Selenium nanoparticles were coupled to the active sites of the proteins LasI (Phe105 and Thr121)/RhII (Leu102 and val138), LasR (Lys42, Arg122, and Glu124)/RhIR (Tyr43, Tyr45, and His61), and MvfR (Leu208 and Arg209). Consequently, nanoparticle-based attenuation of QS in *P. aeruginosa* can be a countermeasure substitute to conventional antibiotics for the therapeutic management of these bacterial infections. Overall, the *in silico* results demonstrate that SeNPs can prevent bacterial infections and may be a potential target for suppressing *P. aeruginosa* QS-mediated pathogenicity and can be designed in several ways to combat bacterial virulence at a feasible cost. However, these anti-QS medications require more in-depth studies before they can be administered in patients. In addition, gene expression analysis along with *in vitro* and *in vivo* experiments such as biocompatibility, cell toxicity, and clinical investigations are prospective research questions which needs to be probed and studied, to determine the efficacy and dosage of SeNPs, before administering in *P. aeruginosa*-infected persons.



## Data availability statement

The original contributions presented in the study are included in the article; further inquiries can be directed to the corresponding author.

## Author contributions

This research was designed by KRK and RSD. KRK carried out the analysis and assessed the findings and wrote the manuscript. RSD and AP read, studied, and amended the draft extensively before finalizing the document. All authors contributed to the article and approved the submitted version.

## Acknowledgments

The authors express their appreciation to the Department of Bioinformatics, Pondicherry University, for providing infrastructure

## References

- Abinaya, M., and Gayathri, M. (2019). Inhibition of biofilm formation, quorum sensing activity and molecular docking study of isolated 3, 5, 7-Trihydroxyflavone from *Alstonia scholaris* leaf against *P. aeruginosa*. *Bioorg. Chem.* 87, 291–301. doi:10.1016/j.bioorg.2019.03.050
- Al-Shabib, N. A., Husain, F. M., Ahmad, N., Qais, F. A., Khan, A., Khan, A., et al. (2018). Facile synthesis of tin oxide hollow nanoflowers interfering with quorum sensing-regulated functions and bacterial biofilms. *J. Nanomater.* 2018, 1–11. doi:10.1155/2018/6845026
- Ali, S. G., Ansari, M. A., Jamal, S., Mohd, Q., Khan, H. M., Jalal, M., et al. (2017). Antiquorum sensing activity of silver nanoparticles in *P. aeruginosa*: an *in silico* study. *Silico Pharmacol.* 5, 1–7. doi:10.1007/s40203-017-0031-3
- Alvarez, M. V., Moreira, M. R., and Ponce, A. (2012). Antiquorum sensing and antimicrobial activity of natural agents with potential use in food. *J. Food Saf.* 32, 379–387. doi:10.1111/j.1745-4565.2012.00390.x
- Arthur, J. R. (1991). The role of selenium in thyroid hormone metabolism. *Can. J. Physiol. Pharmacol.* 69, 1648–1652. doi:10.1139/y91-243
- Balaban, N. Q., Gerdes, K., Lewis, K., and McKinney, J. D. (2013). A problem of persistence: still more questions than answers? *Nat. Rev. Microbiol.* 11, 587–591. doi:10.1038/nrmicro3076
- Banik, S. K., Fenley, A. T., and Kulkarni, R. V. (2009). A model for signal transduction during quorum sensing in *Vibrio harveyi*. *Phys. Biol.* 6, 046008. doi:10.1088/1478-3975/6/4/046008
- Bottomley, M. J., Muraglia, E., Bazzo, R., and Carfi, A. (2007). Molecular insights into quorum sensing in the human pathogen *Pseudomonas aeruginosa* from the structure of the virulence regulator LasR bound to its autoinducer. *J. Biol. Chem.* 282, 13592–13600. doi:10.1074/jbc.M700556200
- Breidenstein, E. B. M., de la Fuente-Núñez, C., and Hancock, R. E. W. (2011). *Pseudomonas aeruginosa*: all roads lead to resistance. *Trends Microbiol.* 19, 419–426. doi:10.1016/j.tim.2011.04.005
- Chatterjee, M., Anju, C. P., Biswas, L., Kumar, V. A., Mohan, C. G., and Biswas, R. (2016). Antibiotic resistance in *Pseudomonas aeruginosa* and alternative therapeutic options. *Int. J. Med. Microbiol.* 306, 48–58. doi:10.1016/j.ijmm.2015.11.004
- Chen, H., Hu, X., Hu, Y., Zhou, J., and Chen, M. (2022). CoVM2: molecular biological data integration of SARS-CoV-2 proteins in a macro-to-micro method. *Biomolecules* 12, 1067. doi:10.3390/biom12081067
- Cornelis, P. (2020). Putting an end to the *Pseudomonas aeruginosa* IQS controversy. *Microbiologyopen* 9, e962. doi:10.1002/mbo3.962
- Davies, D. (2003). Understanding biofilm resistance to antibacterial agents. *Nat. Rev. Drug Discov.* 2, 114–122. doi:10.1038/nrd1008
- DeLano, W. L. (2002). Pymol: an open-source molecular graphics tool. *CCP4 Newsl. Protein Crystallogr.* 40, 82–92.
- Dézil, E., Gopalan, S., Tampakaki, A. P., Lépine, F., Padfield, K. E., Saucier, M., et al. (2005). The contribution of MvfR to *Pseudomonas aeruginosa* pathogenesis and quorum sensing circuitry regulation: multiple quorum sensing-regulated genes are modulated without affecting lasRI, rhlRI or the production of N-acyl-L-homoserine lactones. *Mol. Microbiol.* 55, 998–1014. doi:10.1111/j.1365-2958.2004.04448.x
- Drenkard, E. (2003). Antimicrobial resistance of *Pseudomonas aeruginosa* biofilms. *Microbes Infect.* 5, 1213–1219. doi:10.1016/j.micinf.2003.08.009
- Dubern, J. F., and Diggle, S. P. (2008). Quorum sensing by 2-alkyl-4-quinolones in *Pseudomonas aeruginosa* and other bacterial species. *Mol. Biosyst.* 4, 882–888. doi:10.1039/b803796p
- Dye, C. (2014). After 2015: infectious diseases in a new era of health and development. *Philos. Trans. R. Soc. B Biol. Sci.* 369, 20130426. doi:10.1098/rstb.2013.0426
- Flockton, T. R., Schnorbus, L., Araujo, A., Adams, J., Hammel, M., and Perez, L. J. (2019). Inhibition of *Pseudomonas aeruginosa* biofilm formation with surface modified polymeric nanoparticles. *Pathogens* 8, 55. doi:10.3390/pathogens8020055
- Gellatly, S. L., and Hancock, R. E. W. (2013). *Pseudomonas aeruginosa*: new insights into pathogenesis and host defenses. *Pathog. Dis.* 67, 159–173. doi:10.1111/2049-632X.12033
- Goldsztejn, G., Mundlapati, V. R., Brenner, V., Gloaguen, E., and Mons, M. (2022). Selenium in proteins: conformational changes induced by Se substitution on methionine, as studied in isolated model peptides by optical spectroscopy and quantum chemistry. *Molecules* 27, 3163. doi:10.3390/molecules27103163
- Gómez-Gómez, B., Arregui, L., Serrano, S., Santos, A., Pérez-Corona, T., and Madrid, Y. (2019). Selenium and tellurium-based nanoparticles as interfering factors in quorum sensing-regulated processes: violacein production and bacterial biofilm formation. *Metalomics* 11, 1104–1114. doi:10.1039/c9mt00044e
- Gould, T. A., Schweizer, H. P., and Churchill, M. E. A. (2004). Structure of the *Pseudomonas aeruginosa* acyl-homoserine lactone synthase LasI. *Mol. Microbiol.* 53, 1135–1146. doi:10.1111/j.1365-2958.2004.04211.x
- Gunti, L., Dass, R. S., and Kalagatur, N. K. (2019). Phytofabrication of selenium nanoparticles from *Emblica officinalis* fruit extract and exploring its biopotential applications: antioxidant, antimicrobial, and biocompatibility. *Front. Microbiol.* 10, 931. doi:10.3389/fmicb.2019.00931
- Han, Y., Zhang, J., Hu, C. Q., Zhang, X., Ma, B., and Zhang, P. (2019). *In silico* ADME and toxicity prediction of ceftazidime and its impurities. *Front. Pharmacol.* 10, 434. doi:10.3389/fphar.2019.00434
- Hodgkinson, J. T., Galloway, W. R. J. D., Wright, M., Mati, I. K., Nicholson, R. L., Welch, M., et al. (2012). Design, synthesis and biological evaluation of non-natural modulators of quorum sensing in *Pseudomonas aeruginosa*. *Org. Biomol. Chem.* 10, 6032–6044. doi:10.1039/c2ob25198a
- Hollingsworth, S. A., and Karplus, P. A. (2010). A fresh look at the Ramachandran plot and the occurrence of standard structures in proteins. *Biomol. Concepts* 1, 271–283. doi:10.1515/BMC.2010.022
- Hurley, M. N., Cámará, M., and Smyth, A. R. (2012). Novel approaches to the treatment of *Pseudomonas aeruginosa* infections in cystic fibrosis. *Eur. Respir. J.* 40, 1014–1023. doi:10.1183/09031936.00042012
- Ilangovan, A., Fletcher, M., Rampioni, G., Pustelny, C., Rumbaugh, K., Heeb, S., et al. (2013). Structural basis for native agonist and synthetic inhibitor recognition by the

- Pseudomonas aeruginosa* quorum sensing regulator PqsR (MvfR). *PLoS Pathog.* 9, e1003508. doi:10.1371/journal.ppat.1003508
- Jensen, P. Ø., Bjarnsholt, T., Phipps, R., Rasmussen, T. B., Calum, H., Christoffersen, L., et al. (2007). Rapid necrotic killing of polymorphonuclear leukocytes is caused by quorum-sensing-controlled production of rhamnolipid by *Pseudomonas aeruginosa*. *Microbiology* 153, 1329–1338. doi:10.1099/mic.0.2006/003863-0
- Juan, C., Zamorano, L., Pérez, J. L., Ge, Y., and Oliver, A. (2010). Activity of a new antipseudomonal cephalosporin, CXA-101 (FR264205), against carbapenem-resistant and multidrug-resistant *Pseudomonas aeruginosa* clinical strains. *Antimicrob. Agents Chemother.* 54, 846–851. doi:10.1128/AAC.00834-09
- Killough, M., Rodgers, A. M., and Ingram, R. J. (2022). *Pseudomonas aeruginosa*: recent advances in vaccine development. *Vaccines* 10, 1100. doi:10.3390/vaccines10071100
- Kolodkin-Gal, I., Romero, D., Cao, S., Clardy, J., Kolter, R., and Losick, R. (2010). D-amino acids trigger biofilm disassembly. *Sci.* 328, 627–629. doi:10.1126/science.1188628
- Lansbury, L., Lim, B., Baskaran, V., and Lim, W. S. (2020). Co-Infections in people with COVID-19: a systematic review and meta-analysis. *J. Infect.* 81, 266–275. doi:10.1016/j.jinf.2020.05.046
- Laskowski, R. A., MacArthur, M. W., Moss, D. S., and Thornton, J. M. (1993). Procheck: a program to check the stereochemical quality of protein structures. *J. Appl. Crystallogr.* 26, 283–291. doi:10.1107/s002188992009944
- Lee, J., Wu, J., Deng, Y., Wang, J., Wang, C., Wang, J., et al. (2013). A cell-cell communication signal integrates quorum sensing and stress response. *Nat. Chem. Biol.* 9, 339–343. doi:10.1038/nchembio.1225
- Lee, J., and Zhang, L. (2015). The hierarchy quorum sensing network in *Pseudomonas aeruginosa*. *Protein Cell.* 6, 26–41. doi:10.1007/s13238-014-0100-x
- Lidor, O., Al-Quntar, A., Pesci, E. C., and Steinberg, D. (2015). Mechanistic analysis of a synthetic inhibitor of the *Pseudomonas aeruginosa* LasI quorum-sensing signal synthase. *Sci. Rep.* 5, 16569. doi:10.1038/srep16569
- Lin, J., and Cheng, J. (2019). “Quorum sensing in *Pseudomonas aeruginosa* and its relationship to biofilm development,” in *Introduction to biofilm engineering* (Washington, DC: American Chemical Society), Vol. 1323, 1–16. doi:10.1021/bk-2019-1323.ch001
- Longo, F., Rampioni, G., Bondi, R., Imperi, F., Fimia, G. M., Visca, P., et al. (2013). A new transcriptional repressor of the *Pseudomonas aeruginosa* quorum sensing receptor gene lasR. *PLoS One* 8, e69554. doi:10.1371/journal.pone.0069554
- Lüthy, R., Bowie, J. U., and Eisenberg, D. (1992). Assessment of protein models with three-dimensional profiles. *Nature* 356, 83–85. doi:10.1038/356083a0
- Moker, N., Dean, C. R., and Tao, J. (2010). *Pseudomonas aeruginosa* increases formation of multidrug-tolerant persister cells in response to quorum-sensing signaling molecules. *J. Bacteriol.* 192, 1946–1955. doi:10.1128/JB.101231-09
- Maisonneuve, E., and Gerdes, K. (2014). Molecular mechanisms underlying bacterial persisters. *Cell.* 157, 539–548. doi:10.1016/j.cell.2014.02.050
- Maisuria, V. B., Los Santos, Y. L., Tufenkji, N., and Déziel, E. (2016). Cranberry-derived proanthocyanidins impair virulence and inhibit quorum sensing of *Pseudomonas aeruginosa*. *Sci. Rep.* 6, 30169. doi:10.1038/srep30169
- Matos, E. C. O. D., Andriolo, R. B., Rodrigues, Y. C., Lima, P. D. L. D., Carneiro, I. C., do, R. S., et al. (2018). Mortality in patients with multidrug-resistant *Pseudomonas aeruginosa* infections: a meta-analysis. *Rev. Soc. Bras. Med. Trop.* 51, 415–420. doi:10.1590/0037-8682-0506-2017
- Mishra, A., and Mishra, N. (2021). Antiquorum sensing activity of copper nanoparticle in *Pseudomonas aeruginosa*: an *in silico* approach. *Proc. Natl. Acad. Sci. India Sect. B Biol. Sci.* 91, 29–35. doi:10.1016/j.mib.2021.05.012
- Mlynarcik, P., and Kolar, M. (2017). Starvation-and antibiotics-induced formation of persister cells in *Pseudomonas aeruginosa*. *Biomed. Pap. Med. Fac. Palacky. Univ. Olomouc* 161, 58–67. doi:10.5507/bp.2016.057
- Moghaddam, M. M., Khodi, S., and Mirhosseini, A. (2014). Quorum sensing in bacteria and a glance on *Pseudomonas aeruginosa*. *Clin. Microb.* 3 (4), 156. doi:10.4172/2327-5073.1000156
- Moradali, M. F., Ghods, S., and Rehm, B. H. A. (2017). *Pseudomonas aeruginosa* lifestyle: a paradigm for adaptation, survival, and persistence. *Front. Cell. Infect. Microbiol.* 7, 39. doi:10.3389/fcimb.2017.00039
- Mühling, M., Bradford, A., Readman, J. W., Somerfield, P. J., and Handy, R. D. (2009). An investigation into the effects of silver nanoparticles on antibiotic resistance of naturally occurring bacteria in an estuarine sediment. *Mar. Environ. Res.* 68, 278–283. doi:10.1016/j.marenvres.2009.07.001
- Nafee, N., Husari, A., Maurer, C. K., Lu, C., de Rossi, C., Steinbach, A., et al. (2014). Antibiotic-free nanotherapeutics: ultra-small, mucus-penetrating solid lipid nanoparticles enhance the pulmonary delivery and anti-virulence efficacy of novel quorum sensing inhibitors. *J. Control. Release* 192, 131–140. doi:10.1016/j.jconrel.2014.06.055
- Osmon, S., Ward, S., Fraser, V. J., and Kollef, M. H. (2004). Hospital mortality for patients with bacteremia due to *Staphylococcus aureus* or *Pseudomonas aeruginosa*. *Chest* 125, 607–616. doi:10.1378/chest.125.2.607
- Paczkowski, J. E., McCready, A. R., Cong, J. P., Li, Z., Jeffrey, P. D., Smith, C. D., et al. (2019). An autoinducer analogue reveals an alternative mode of ligand binding for the LasR quorum-sensing receptor. *ACS Chem. Biol.* 14, 378–389. doi:10.1021/acscchembio.8b00971
- Pal, S., Tak, Y. K., and Song, J. M. (2007). Does the antibacterial activity of silver nanoparticles depend on the shape of the nanoparticle? A study of the gram-negative bacterium *Escherichia coli*. *Appl. Environ. Microbiol.* 73, 1712–1720. doi:10.1128/AEM.02218-06
- Pang, Z., Raudonis, R., Glick, B. R., Lin, T. J., and Cheng, Z. (2019). Antibiotic resistance in *Pseudomonas aeruginosa*: mechanisms and alternative therapeutic strategies. *Biotechnol. Adv.* 37, 177–192. doi:10.1016/j.biotechadv.2018.11.013
- Parai, D., Banerjee, M., Dey, P., Chakraborty, A., Islam, E., and Mukherjee, S. K. (2018). Effect of reserpine on *Pseudomonas aeruginosa* quorum sensing mediated virulence factors and biofilm formation. *Biofouling* 34, 320–334. doi:10.1080/08927014.2018.1437910
- Passador, L., Cook, J. M., Gambello, M. J., Rust, L., and Iglewski, B. H. (1993). Expression of *Pseudomonas aeruginosa* virulence genes requires cell-to-cell communication. *Sci.* 260, 1127–1130. doi:10.1126/science.8493556
- Pearson, J. P., Pesci, E. C., and Iglewski, B. H. (1997). Roles of *Pseudomonas aeruginosa* las and rhl quorum-sensing systems in control of elastase and rhamnolipid biosynthesis genes. *J. Bacteriol.* 179, 5756–5767. doi:10.1128/jb.179.18.5756-5767.1997
- Pesci, E. C., Milbank, J. B. J., Pearson, J. P., McKnight, S., Kende, A. S., Greenberg, E. P., et al. (1999). Quinolone signaling in the cell-to-cell communication system of *Pseudomonas aeruginosa*. *Proc. Natl. Acad. Sci.* 96, 11229–11234. doi:10.1073/pnas.96.20.11229
- Qin, S., Xiao, W., Zhou, C., Pu, Q., Deng, X., Lan, L., et al. (2022). *Pseudomonas aeruginosa*: pathogenesis, virulence factors, antibiotic resistance, interaction with host, technology advances and emerging therapeutics. *Signal Transduct. Target. Ther.* 7, 199. doi:10.1038/s41392-022-01056-1
- Raman, G., Avendano, E. E., Chan, J., Merchant, S., and Puzniak, L. (2018). Risk factors for hospitalized patients with resistant or multidrug-resistant *Pseudomonas aeruginosa* infections: a systematic review and meta-analysis. *Antimicrob. Resist. Infect. Control* 7, 79–14. doi:10.1186/s13756-018-0370-9
- Raman, S., Vernon, R., Thompson, J., Tyka, M., Sadreyev, R., Pei, J., et al. (2009). Structure prediction for CASP8 with all-atom refinement using Rosetta. *Proteins Struct. Funct. Bioinforma.* 77, 89–99. doi:10.1002/prot.22540
- Rampioni, G., Falcone, M., Heeb, S., Frangipani, E., Fletcher, M. P., Dubern, J. F., et al. (2016). Unravelling the genome-wide contributions of specific 2-alkyl-4-quinolones and PqsE to quorum sensing in *Pseudomonas aeruginosa*. *PLoS Pathog.* 12, e1006029. doi:10.1371/journal.ppat.1006029
- Rathinam, P., Vijay Kumar, H. S., and Viswanathan, P. (2017). Eugenol exhibits anti-virulence properties by competitively binding to quorum sensing receptors. *Biofouling* 33, 624–639. doi:10.1080/08927014.2017.1350655
- Rayman, M. P. (2005). Selenium in cancer prevention: a review of the evidence and mechanism of action. *Proc. Nutr. Soc.* 64, 527–542. doi:10.1079/pns2005467
- Reading, N. C., and Sperandio, V. (2006). Quorum sensing: the many languages of bacteria. *FEMS Microbiol. Lett.* 254, 1–11. doi:10.1111/j.1574-6968.2005.00001.x
- Reis, R. S., Pereira, A. G., Neves, B. C., and Freire, D. M. (2011). Gene regulation of rhamnolipid production in *Pseudomonas aeruginosa*—a review. *Bioresour. Technol.* 102 (11), 6377–6384. doi:10.1016/j.biortech.2011.03.074
- Reuter, K., Steinbach, A., and Helms, V. (2016). Interfering with bacterial quorum sensing. *Perspect. Med. Chem.* 8, 1–15. doi:10.4137/PMC.S13209
- Rotruck, J. T., Pope, A. L., Ganther, H. E., Swanson, A. B., Hafeman, D. G., and Hoekstra, W. (1973). Selenium: biochemical role as a component of glutathione peroxidase. *Science* 179, 588–590. doi:10.1126/science.179.4073.588
- Rutherford, S. T., and Bassler, B. L. (2012). Bacterial quorum sensing: its role in virulence and possibilities for its control. *Cold Spring Harb. Perspect. Med.* 2, a012427. doi:10.1101/cshperspect.a012427
- Samanta, S., Singh, B. R., and Adholeya, A. (2017). Intracellular synthesis of gold nanoparticles using an ectomycorrhizal strain EM-1083 of *Laccaria fraterna* and its nanoanti-quorum sensing potential against *Pseudomonas aeruginosa*. *Indian J. Microbiol.* 57, 448–460. doi:10.1007/s12088-017-0662-4
- Sandoval-Motta, S., and Aldana, M. (2016). Adaptive resistance to antibiotics in bacteria: a systems biology perspective. *Wiley Interdiscip. Rev. Syst. Biol. Med.* 8, 253–267. doi:10.1002/wsbm.1335
- Schneidman-Duhovny, D., Inbar, Y., Nussinov, R., and Wolfson, H. J. (2005). PatchDock and SymmDock: servers for rigid and symmetric docking. *Nucleic Acids Res.* 33, W363–W367. doi:10.1093/nar/gki481
- Shah, S., Gaikwad, S., Nagar, S., Kulshrestha, S., Vaidya, V., Nawani, N., et al. (2019). Biofilm inhibition and anti-quorum sensing activity of phytosynthesized silver nanoparticles against the nosocomial pathogen *Pseudomonas aeruginosa*. *Biofouling* 35, 34–49. doi:10.1080/08927014.2018.1563686
- Shepp, D. H., Tang, I. T., Ramundo, M. B., and Kaplan, M. K. (1994). Serious *Pseudomonas aeruginosa* infection in AIDS. *J. Acquir. Immune Defic. Syndr.* 7, 823–831.

- Shin, D., Gorgulla, C., Boursier, M. E., Rexrode, N., Brown, E. C., Arthanari, H., et al. (2019). N-acyl homoserine lactone analog modulators of the *Pseudomonas aeruginosa* RhII quorum sensing signal synthase. *ACS Chem. Biol.* 14, 2305–2314. doi:10.1021/acscchembio.9b00671
- Simanek, K. A., Taylor, I. R., Richael, E. K., Lasek-Nesselquist, E., Bassler, B. L., and Paczkowski, J. E. (2022). The PqsE-RhIR interaction regulates RhIR DNA binding to control virulence factor production in *Pseudomonas aeruginosa*. *Microbiol. Spectr.* 10(1), e02108-21. doi:10.1128/spectrum.02108-21
- Singh, B. R., Shoeb, M., Sharma, S., Naqvi, A. H., Gupta, V. K., Singh, B. N., et al. (2017). Scaffold of selenium nanovectors and honey phytochemicals for inhibition of *Pseudomonas aeruginosa* quorum sensing and biofilm formation. *Front. Cell. Infect. Microbiol.* 7, 93. doi:10.3389/fcimb.2017.00093
- Smith, R. S., and Iglewski, B. H. (2003). *P. aeruginosa* quorum-sensing systems and virulence. *Curr. Opin. Microbiol.* 6, 56–60. doi:10.1016/s1369-5274(03)00008-0
- Song, Y., DiMaio, F., Wang, R. Y. R., Kim, D., Miles, C., Brunette, T. J., et al. (2013). High-resolution comparative modeling with RosettaCM. *Structure* 21, 1735–1742. doi:10.1016/j.str.2013.08.005
- Stewart, P. S. (2002). Mechanisms of antibiotic resistance in bacterial biofilms. *Int. J. Med. Microbiol.* 292, 107–113. doi:10.1078/1438-4221-00196
- Strateva, T., and Mitov, I. (2011). Contribution of an arsenal of virulence factors to pathogenesis of *Pseudomonas aeruginosa* infections. *Ann. Microbiol.* 61, 717–732. doi:10.1007/s13213-011-0273-y
- Su, H. C., Ramkissoon, K., Doolittle, J., Clark, M., Khatun, J., Secrest, A., et al. (2010). The development of ciprofloxacin resistance in *Pseudomonas aeruginosa* involves multiple response stages and multiple proteins. *Antimicrob. Agents Chemother.* 54, 4626–4635. doi:10.1128/AAC.00762-10
- Taylor, P. K., Yeung, A. T. Y., and Hancock, R. E. W. (2014). Antibiotic resistance in *Pseudomonas aeruginosa* biofilms: towards the development of novel anti-biofilm therapies. *J. Biotechnol.* 191, 121–130. doi:10.1016/j.jbiotec.2014.09.003
- Tran, P. A., O'Brien-Simpson, N., Reynolds, E. C., Pantarat, N., Biswas, D. P., and O'Connor, A. J. (2015). Low cytotoxic trace element selenium nanoparticles and their differential antimicrobial properties against *S. aureus* and *E. coli*. *Nanotechnology* 27, 045101. doi:10.1088/0957-4484/27/4/045101
- Van Delden, C., and Iglewski, B. H. (1998). Cell-to-cell signaling and *Pseudomonas aeruginosa* infections. *Emerg. Infect. Dis.* 4, 551–560. doi:10.3201/eid0404.980405
- Van Gennip, M., Christensen, L. D., Alhede, M., Phipps, R., Jensen, P. Ø., Christophersen, L., et al. (2009). Inactivation of the rhlA gene in *Pseudomonas aeruginosa* prevents rhamnolipid production, disabling the protection against polymorphonuclear leukocytes. *Apmis* 117, 537–546. doi:10.1111/j.1600-0463.2009.02466.x
- Velmourougane, K., and Prasanna, R. (2017). Influence of l-amino acids on aggregation and biofilm formation in *Azotobacter chroococcum* and *Trichoderma viride*. *J. Appl. Microbiol.* 123, 977–991. doi:10.1111/jam.13534
- Vriend, G. (1990). What if: a molecular modeling and drug design program. *J. Mol. Graph.* 8, 52–56. doi:10.1016/0263-7855(90)80070-v
- Vyshnava, S. S., Kanderi, D. K., Panjala, S. P., Pandian, K., Bontha, R. R., Goukanapalle, P. K. R., et al. (2016). Effect of silver nanoparticles against the formation of biofilm by *Pseudomonas aeruginosa* an *in silico* approach. *Appl. Biochem. Biotechnol.* 180, 426–437. doi:10.1007/s12010-016-2107-7
- Wang, Y., Gao, L., Rao, X., Wang, J., Yu, H., Jiang, J., et al. (2018). Characterization of lasR-deficient clinical isolates of *Pseudomonas aeruginosa*. *Sci. Rep.* 8, 13344. doi:10.1038/s41598-018-30813-y
- Weir, E., Lawlor, A., Whelan, A., and Regan, F. (2008). The use of nanoparticles in anti-microbial materials and their characterization. *Analyst* 133, 835–845. doi:10.1039/b715532h
- Williams, M. E., and Cloete, R. (2022). Molecular modeling of subtype-specific Tat protein signatures to predict Tat-TAR interactions that may be involved in HIV-associated neurocognitive disorders. *Front. Microbiol.* 13, 866611. doi:10.3389/fmicb.2022.866611
- Wood, S. J., Kuzel, T. M., and Shafikhani, S. H. (2023). *Pseudomonas aeruginosa*: infections, animal modeling, and therapeutics. *Cells* 12, 199. doi:10.3390/cells12010199
- Yin, I. X., Zhang, J., Zhao, I. S., Mei, M. L., Li, Q., and Chu, C. H. (2020). The antibacterial mechanism of silver nanoparticles and its application in dentistry. *Int. J. Nanomedicine* 15, 2555–2562. doi:10.2147/IJN.S246764
- Zou, Y., and Nair, S. K. (2009). Molecular basis for the recognition of structurally distinct autoinducer mimics by the *Pseudomonas aeruginosa* LasR quorum-sensing signaling receptor. *Chem. Biol.* 16, 961–970. doi:10.1016/j.chembiol.2009.09.001